BNL-75079-2005-JA

# Comparison of inclusive particle production in 14.6 GeV/c proton-nucleus collisions with simulation

D. E. Jaffe [b], K. H. Lo [c], J. R. Comfort [a], and M. Sivertz [b]

[a] *Arizona State University, Dept. of Physics and Astronomy, Tempe, AZ*

[b] *Brookhaven National Laboratory, Upton, NY*

[c] *Stony Brook University, Dept. of Physics and Astronomy, Stony Brook, NY*

**Abstract**

Inclusive charged pion, kaon, proton, and deuteron production in 14.6 GeV/c proton-nucleus collisions measured by BNL experiment E802 is compared with results from the GEANT3, GEANT4, and FLUKA simulation packages. The FLUKA package is found to have the best overall agreement.

*Key words:* simulation, Monte Carlo, inclusive production, proton-nucleus collisions
*PACS:* 13.85.Ni, 02.70.Uu, 07.05.Tp

## 1 Introduction

The simulation of particle production in proton-nucleus collisions is important for a number of ongoing and future high energy physics experiments. Interpretation of atmospheric neutrino data requires knowledge of hadronic interactions on light nuclei for lab energies from 1 to $10^5$ GeV [1]. The design of secondary beams for the study of neutrino interactions [2] or rare kaon decay [3] relies on the accurate simulation of proton-nucleus collisions at energies in the range 10-100 GeV. In addition, validation of simulations in accessible energy regions is important for the interpretation of LHC data [4].

In this paper we compare the data of BNL experiment E802 [5] with simulated results of the GEANT3 [6], GEANT4 [7], and FLUKA [8] packages. Experiment E802 measured $\pi^{\pm}$, $K^{\pm}$, proton, and deuteron production in the angular range 5° to 58° in collisions of 14.6 GeV/$c$ protons with Be, Al, Cu,

and Au targets. The E802 magnetic spectrometer had a geometrical solid angle acceptance of 25 msr and was rotated to take data at five overlapping angular settings. Particle identification was accomplished with time-of-flight and a gas Cherenkov detector. The measured spectra were presented as invariant cross sections $\frac{d^2\sigma}{2\pi m_t dm_t dy}$ as a function of transverse kinetic energy $(m_t - m_0)c^2 = \sqrt{(m_0c^2)^2 + (p_\perp c)^2} - m_0c^2$ in bins of rapidity where $m_0$ is the particle mass. The overall uncertainty in the cross section normalization is estimated to be $\pm(10-15)\%$.

The E802 results have previously been compared to simulation. The JAM1.0 hadronic cascade model [9] showed good agreement with the measured proton, $\pi^\pm$, and $K^\pm$ spectra for all four targets as a function of $m_t - m_0$ and rapidity. The $p$-Be data as a function of rapidity has been compared with FLUKA [10] in the calculation of atmospheric neutrino flux. The agreement is reasonable with the largest deviation being a factor $\sim 1.2$ ($\sim 2$) for the pion (kaon) spectra. Several simulation models were compared with the $p$-Be data as a function of $m_t - m_0$ and rapidity in the framework of the CORSIKA program [11]. Pion production in FLUKA 2002 and UrQMD 1.3 [12] had the same slope as function of $m_t - m_0$ as the data over the whole rapidity range, while the GHEISHA 2002 [14], QGSJET 01 [15], and neXus 3 [13] models were unable to reproduce the slope as a function of $m_t - m_0$ over the full kinematic range of the data.

## 2 Simulation packages

In this paper for the GEANT3 simulation we used the hadronic simulation package GCALOR version 1.05/03 [16] with GEANT version 3.21, for the GEANT4 simulation we used GEANT version 4.7.1 and simulation packages ("physics lists") QGSP, QGSC, QGSP_BIC, and QGSC_LEAD_HP [17], and we used version 2005.6 of FLUKA. The GEANT4 physics list QGSP employs a "quark gluon string model... and a pre-equilibrium decay model with an extensive evaporation phase to model the subsequent nuclear fragmentation" and is recommended [17] for medium energy (15-50 GeV) protons on light targets. QGSC is similar to QGSP for the initial reaction and " ...uses chiral invariant phase-space decay ... to model the behavior of the system's fragmentation." QGSP_BIC is similar to QGSP but uses the binary cascade for nucleon interactions below 3 GeV. QGSC and QGSC_BIC are recommended physics lists for high energy applications. The physics list QGSC_LEAD_HP is recommended for the calculation of LHC detector neutron fluxes.

We simulated 14.6 GeV/$c$ proton interactions on Be, Al, Cu, and Au targets of thickness 1478 mg/cm$^2$, 1620 mg/cm$^2$, 1434 mg/cm$^2$, and 1000 mg/cm$^2$,

respectively. The kinematics of charged pions, kaons, protons, and deuterons at a radius of 25 cm from the interaction point were recorded. The lifetime of the charged mesons was artificially set to be infinite to avoid performing a decay-in-flight correction to the measured yields. For each target and model we generated 50 million incident protons. No importance weighting or event biasing was used and the uncertainty in the evaluated cross sections is based on the statistics of the generated events only.

## 3 Comparison with E802 data

The data and simulation results are shown in Figures 1, 2, 3, 4, 5, and 6 for the four targets for $\pi^+$, $\pi^-$, $K^+$, $K^-$, $p$, and $d$ data, respectively. Only the QGSC GEANT4 results are shown for the $\pi^\pm$, $K^\pm$, and $p$ data as the four GEANT4 simulation packages give nearly identical results. For the deuteron data, only the packages that give non-zero cross sections for $y > 0.4$ are shown in Figure 6.

The ratios of Monte Carlo results to data are shown in Figures 7, 8, 9, and 10 for positive pion production on beryllium, aluminum, copper and gold targets, respectively. Similarly, for each target, the ratios for negative pions are shown in Figures 11, 12, 13, and 14, for positive kaons in Figures 15, 16, 17, and 18, for negative kaons in Figures 19, 20, 21, and 22, and for protons in Figures 23, 24, 25, and 26. The ratios are not shown for the deuteron data given the sparse nature and obviously poor agreement with the simulation. The statistical uncertainty in the data and the Monte Carlo are combined in quadrature to produce the uncertainty in the ratios shown in the Figures and the E802 normalization uncertainty is indicated separately.

As seen in Figures 7, 8, 9, and 10 for $\pi^+$ production, FLUKA generally has good agreement in slope but overestimates the magnitude by up to a factor of two at low rapidity. All the GEANT4 packages give similar results and agree in magnitude with the data at lowest $m_\mathrm{t}$ but do not agree in slope for $y < 1.4$, 1.6, 1.6, and 1.8 for the Be, Al, Cu, and Au targets, respectively. GCALOR has better agreement than FLUKA or GEANT4 for the $\pi^+$ data.

Similar observations can be made for $\pi^-$ production in Figures 11, 12, 13, and 14. GCALOR most accurately reproduces the data over the measured kinematic range with some underestimate of the magnitude at low $m_\mathrm{t}$ and high rapidity. FLUKA has reasonable agreement in slope and is within a factor of two in magnitude for all the data. The GEANT4 agreement is good for all the Be data (Figure 11) and agrees for the heavier targets at low $m_\mathrm{t}$ or $y >$ 1.2, 1.6, and 1.6 for Al, Cu, and Au, respectively.

For positive kaon production FLUKA agrees in slope and magnitude for the Al (Figure 16), Cu (Figure 17), and Au (Figure 18) targets. For the Be (Figure 15) target, FLUKA agrees in slope but the magnitude is higher than the data. The GCALOR agreement with the data is comparable to FLUKA for the Be target, but consistently underestimates the magnitude for the heavier targets. All the GEANT4 packages have the wrong slope for all targets and only agree in magnitude at lowest $m_{\mathrm{t}}$.

Both FLUKA and GCALOR reproduce the slope of the $K^-$ data reasonably well (Figures 19, 20, 21, and 22 ). The magnitude predicted by FLUKA is higher than the data, while GCALOR has better agreement. The slope of the Be data is reproduced reasonably well by the GEANT4 packages, but is lower in magnitude than the data. For the heavier targets, GEANT4 predicts a slope less than that of the data and agrees in magnitude only at lowest $m_{\mathrm{t}}$.

For proton production from the Be target (Figure 23), both FLUKA and the GEANT4 packages have a slope greater than that of the data with moderately good agreement with the data in magnitude at low $m_{\mathrm{t}}$. For the heavier targets, FLUKA generally has good agreement for $y < 1.3$, but the predicted slope exceeds the data for larger rapidities. For the GEANT4 packages for the heavier targets, the agreement is poor for $y < 2.2$, 1.6, and 1.6 for Al (Figure 23), Cu (Figure 25), and Au (Figure 26), respectively, but improves somewhat at higher rapidities. In general the slope of the GEANT4 packages does not match the data well over the full range of measured $m_{\mathrm{t}}$. It is notable that the QGSC differs from the other GEANT4 packages only for proton production and for the Au target. GCALOR has the poorest agreement with the data.

None of the simulation packages reproduces the deuteron data (Figure 6) well. Neither GCALOR nor FLUKA predict a significant production of deuterons for rapidity above 0.5. QGSC and QGSC_LEAD_HP underestimate the deuteron rate by an order of magnitude but do a reasonable job at predicting the slope of the deuteron data at low rapidity. The agreement is worse at rapidity greater than $\sim$0.8.

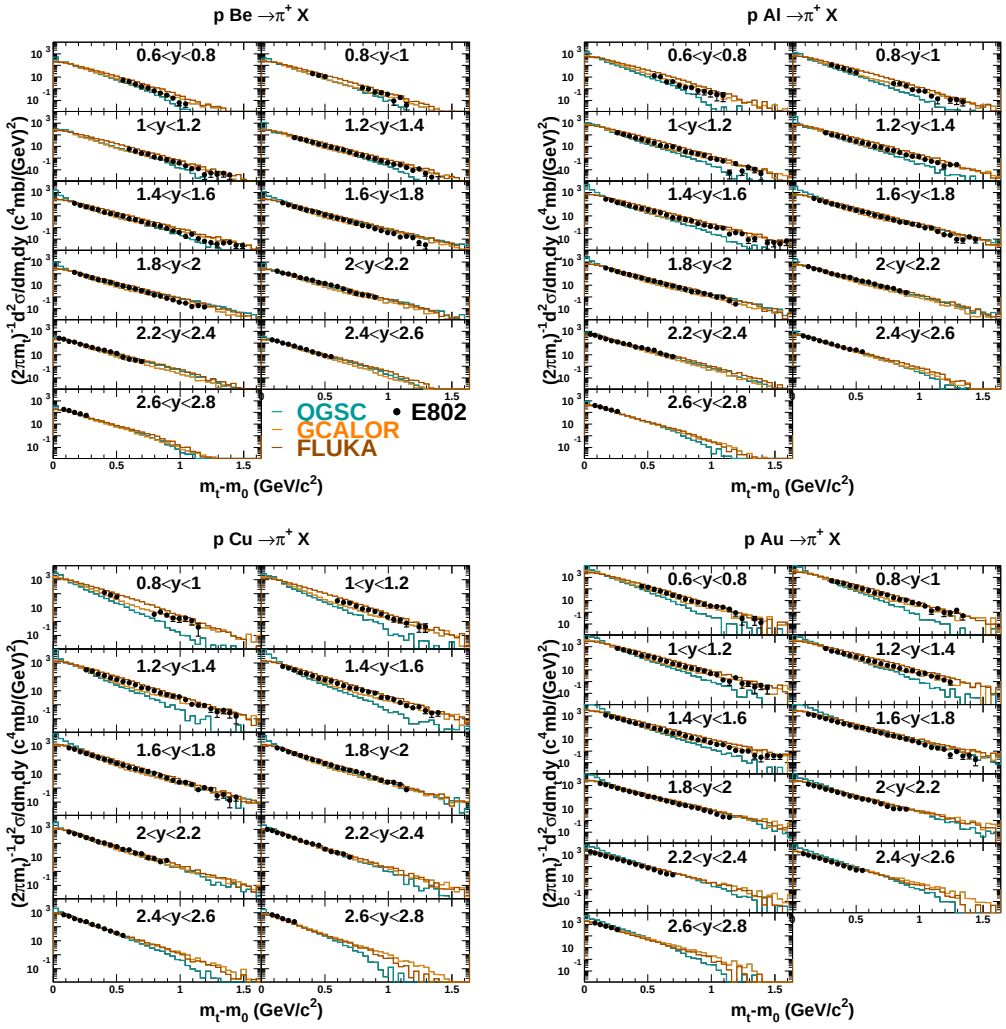


Fig. 1. The invariant cross section $\frac{d^2\sigma}{2\pi m_{\rm t}\, dm_{\rm t}\, dy}$ as a function of transverse kinetic energy $m_{\rm t} - m_0$ in 0.2 bins of rapidity compared to the simulation results for the $\pi^+$ data for $p$-Be, $p$-Al, $p$-Cu, and $p$-Au collisions.

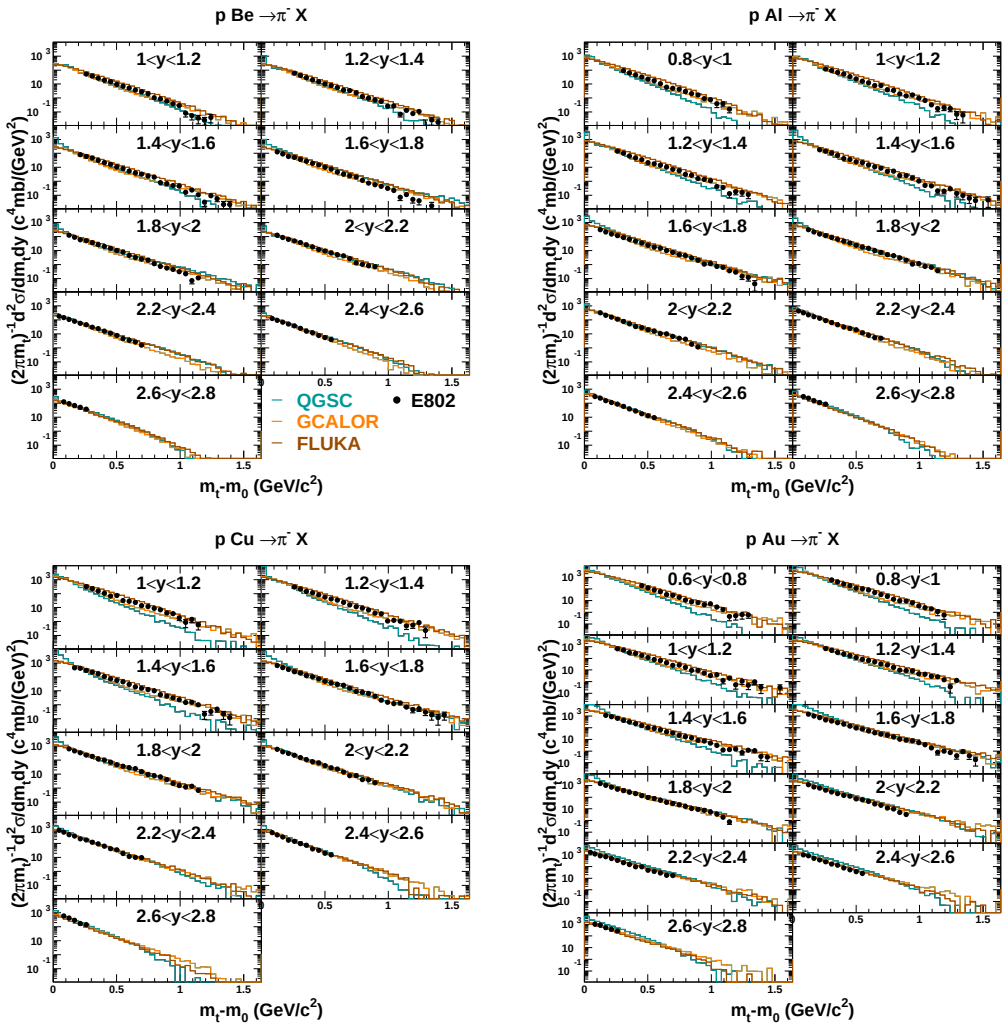


Fig. 2. The invariant cross section $\frac{d^2\sigma}{2\pi m_{\rm t}\, dm_{\rm t}\, dy}$ as a function of transverse kinetic energy $m_{\rm t} - m_0$ in 0.2 bins of rapidity compared to the simulation results for the $\pi^-$ data for $p$-Be, $p$-Al, $p$-Cu, and $p$-Au collisions.

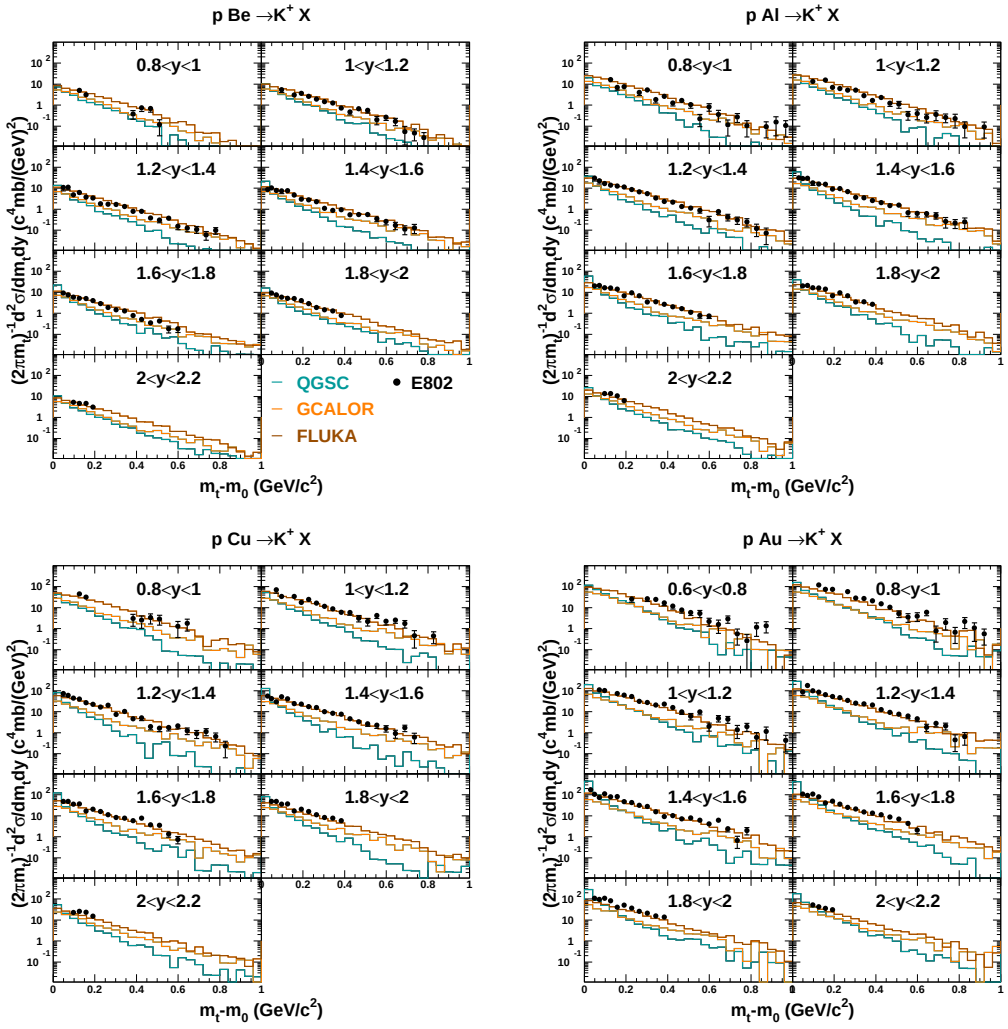


Fig. 3. The invariant cross section $\frac{d^2\sigma}{2\pi m_{\rm t}\, dm_{\rm t}\, dy}$ as a function of transverse kinetic energy $m_{\rm t} - m_0$ in 0.2 bins of rapidity compared to the simulation results for the $K^+$ data for $p$-Be, $p$-Al, $p$-Cu, and $p$-Au collisions.

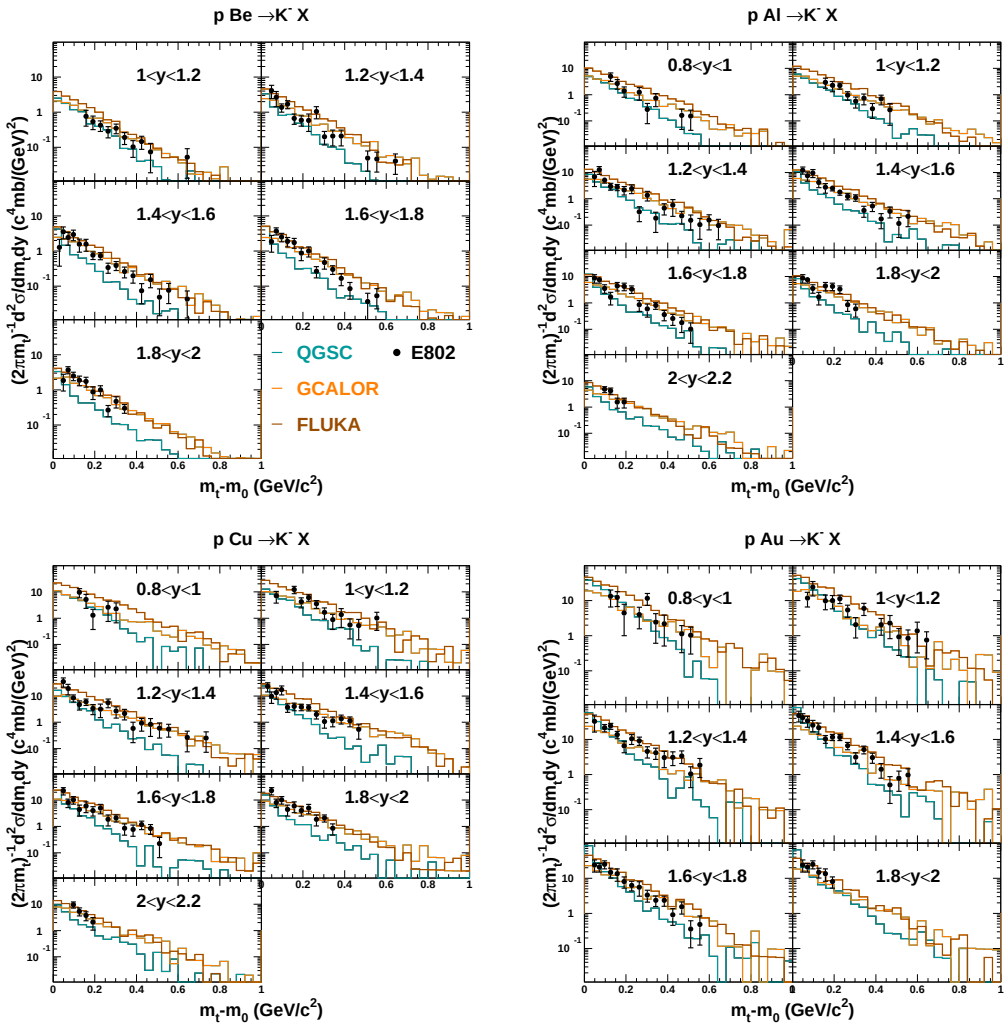


Fig. 4. The invariant cross section $\frac{d^2\sigma}{2\pi m_{\rm t}\, dm_{\rm t}\, dy}$ as a function of transverse kinetic energy $m_{\rm t} - m_0$ in 0.2 bins of rapidity compared to the simulation results for the $K^-$ data for $p$-Be, $p$-Al, $p$-Cu, and $p$-Au collisions.

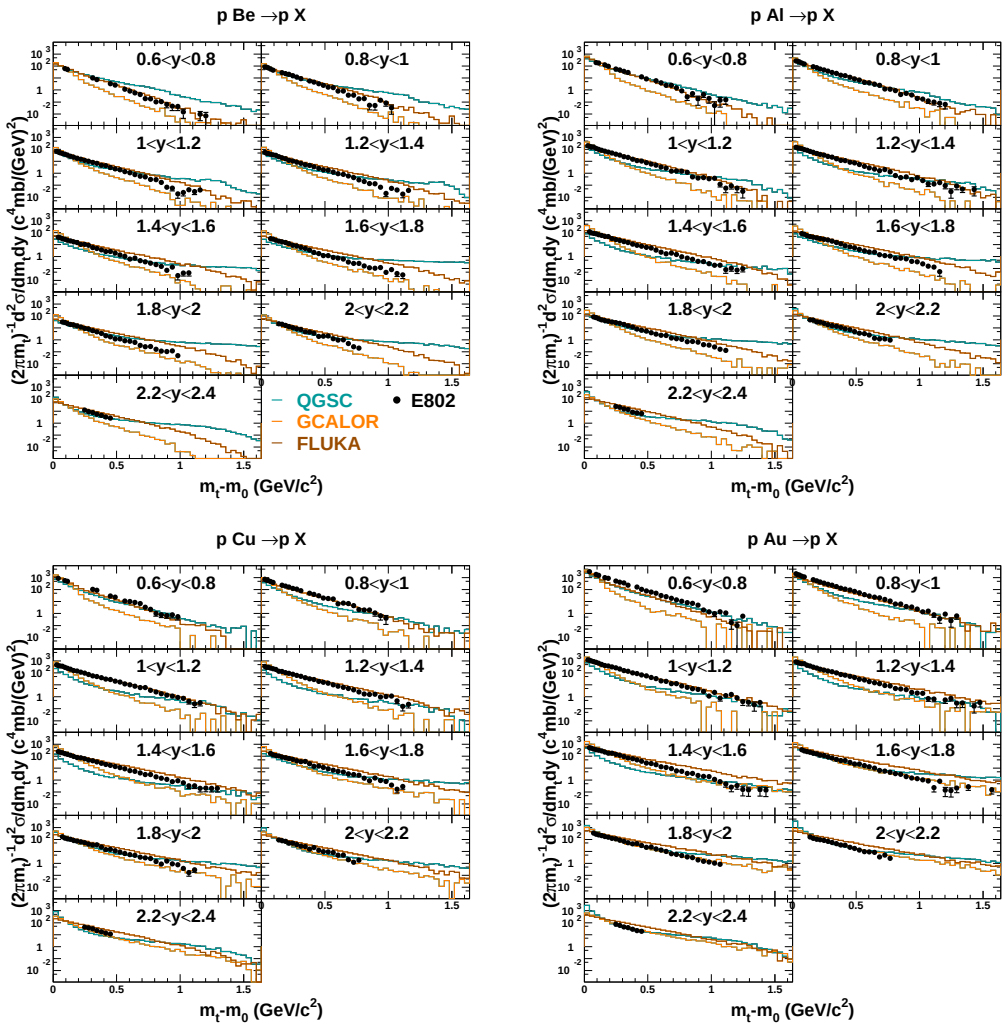


Fig. 5. The invariant cross section $\frac{d^2\sigma}{2\pi m_{\mathrm{t}} dm_{\mathrm{t}} dy}$ as a function of transverse kinetic energy $m_{\mathrm{t}} - m_0$ in 0.2 bins of rapidity compared to the simulation results for the proton data for $p$-Be, $p$-Al, $p$-Cu, and $p$-Au collisions.

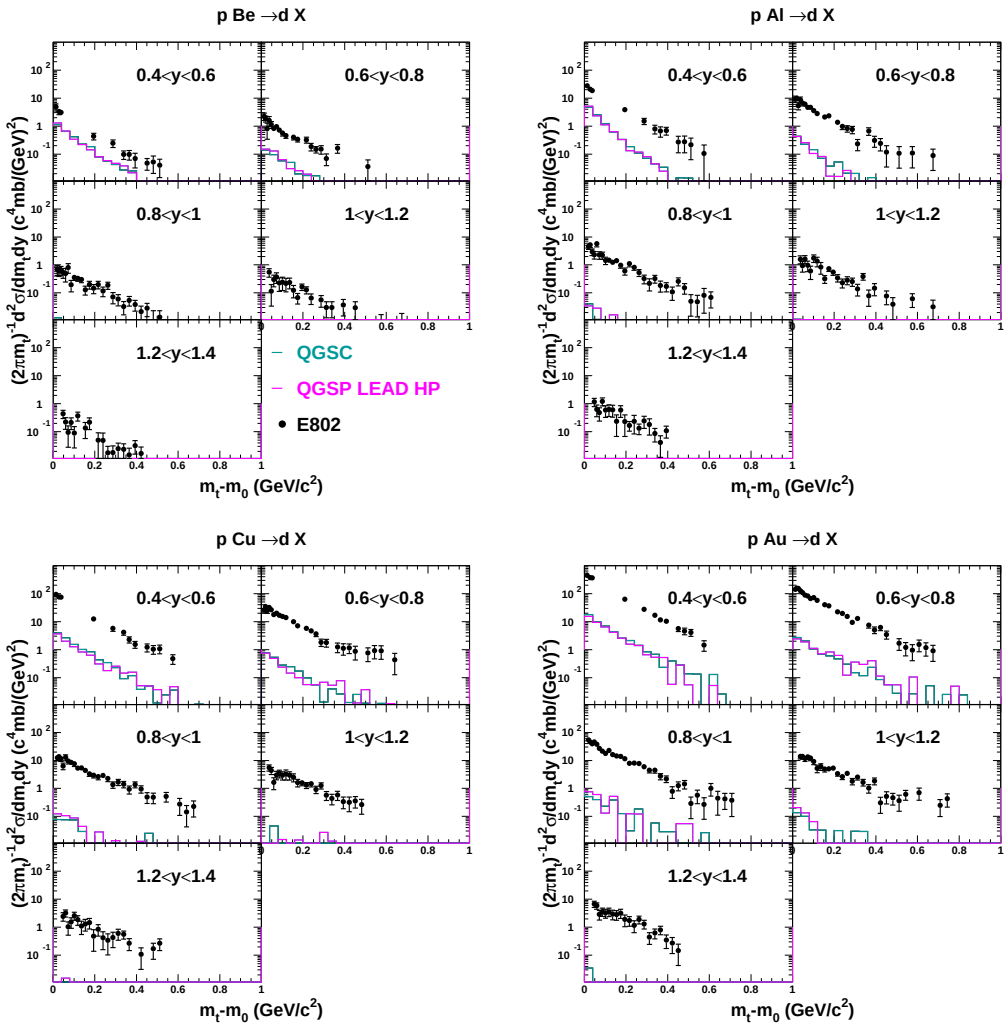


Fig. 6. The invariant cross section $\frac{d^2\sigma}{2\pi m_{\rm t} dm_{\rm t}\, dy}$ as a function of transverse kinetic energy $m_{\rm t} - m_0$ in 0.2 bins of rapidity compared to the simulation results for the deuteron data for $p$-Be, $p$-Al, $p$-Cu, and $p$-Au collisions.

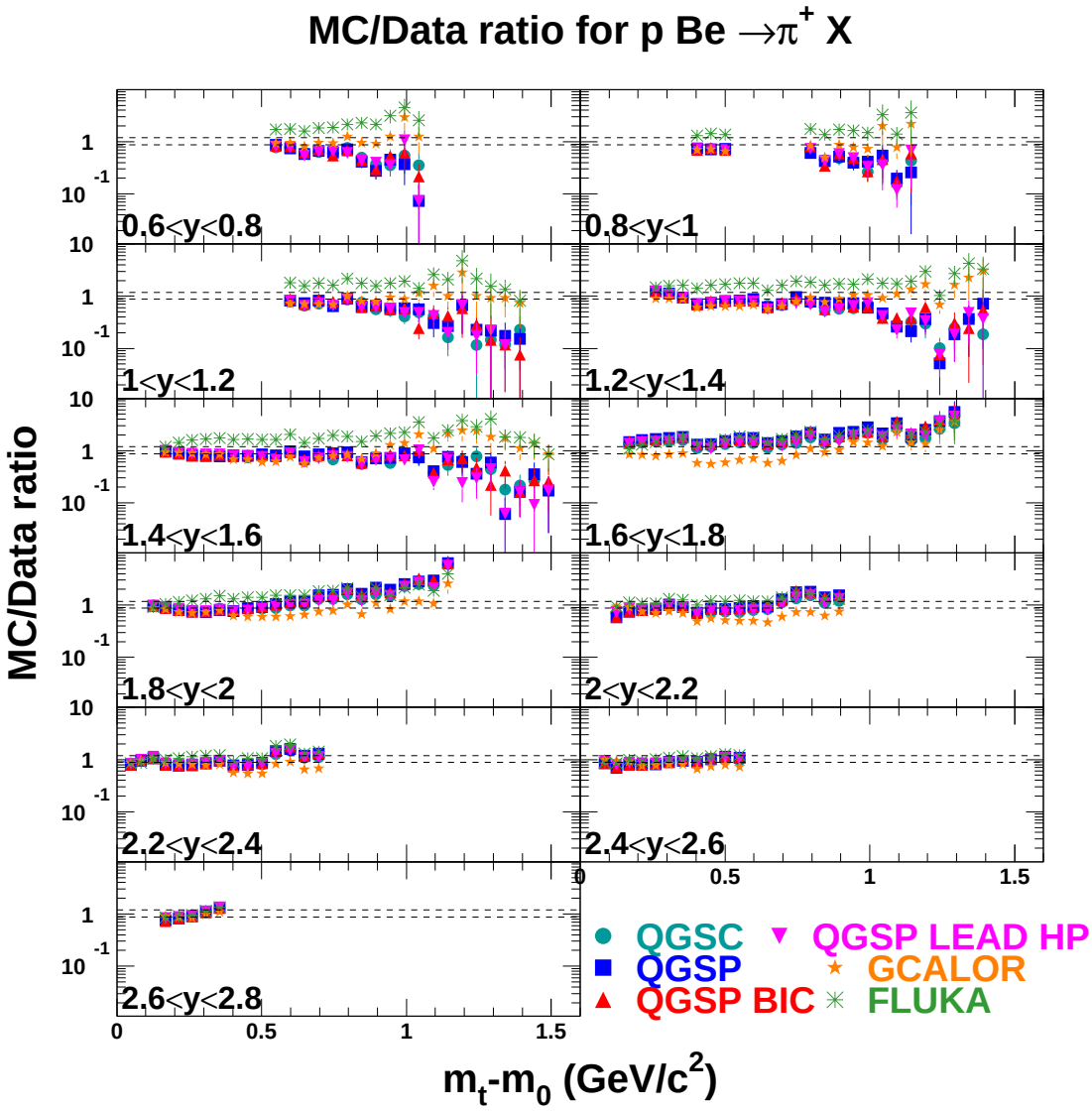


Fig. 7. The ratio of the simulated (MC) and data invariant cross sections as a function of transverse kinetic energy $m_t - m_0$ in 0.2 bins of rapidity for the $\pi^+$ data for $p$-Be collisions. The horizontal dashed lines indicate the $\pm 15\%$ normalization uncertainty of the E802 data.

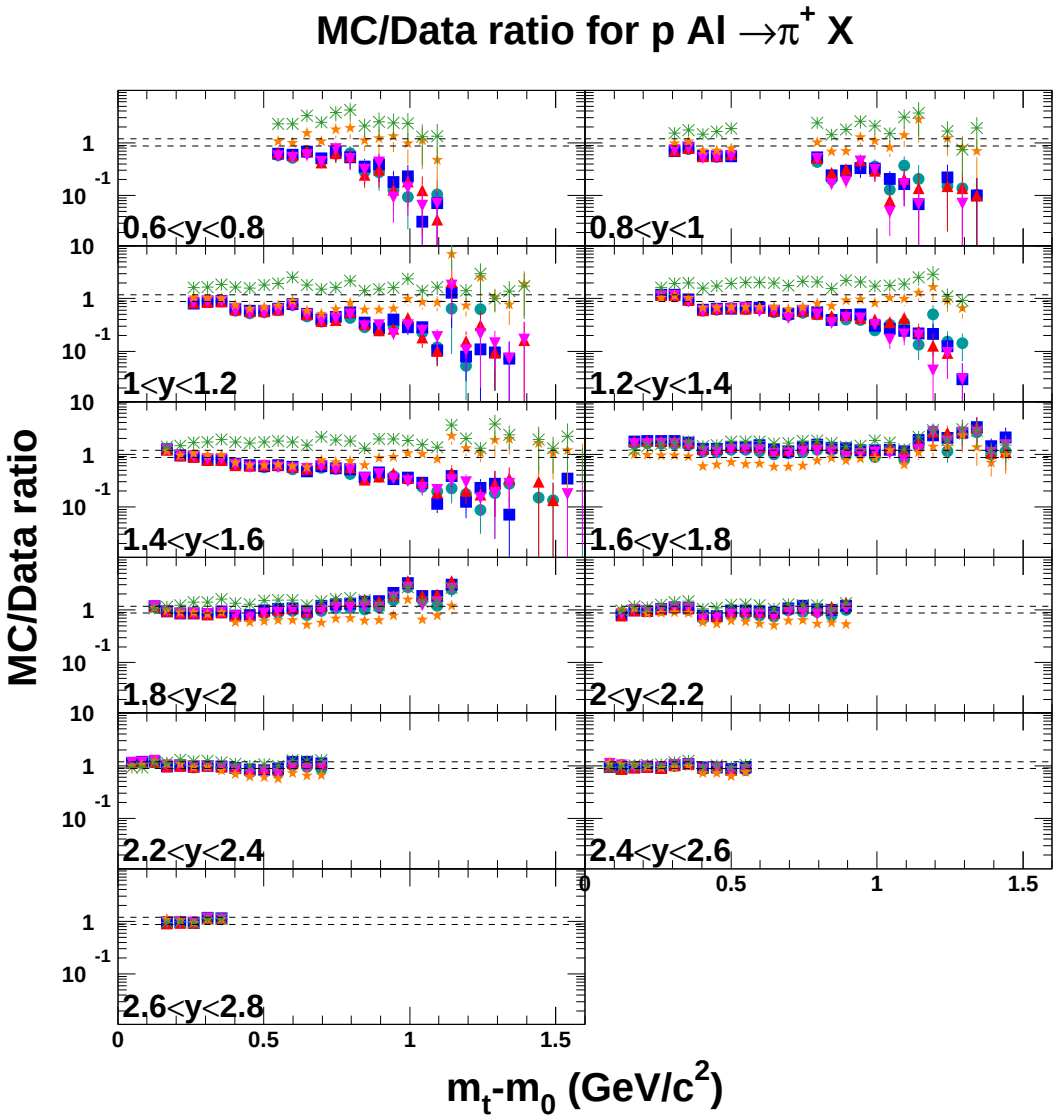


Fig. 8. The ratio of the simulated (MC) and data invariant cross sections as a function of transverse kinetic energy $m_t - m_0$ in 0.2 bins of rapidity for the $\pi^+$ data for $p$-Al collisions. The horizontal dashed lines indicate the $\pm 15\%$ normalization uncertainty of the E802 data. The symbol definitions are the same as Figure 7.

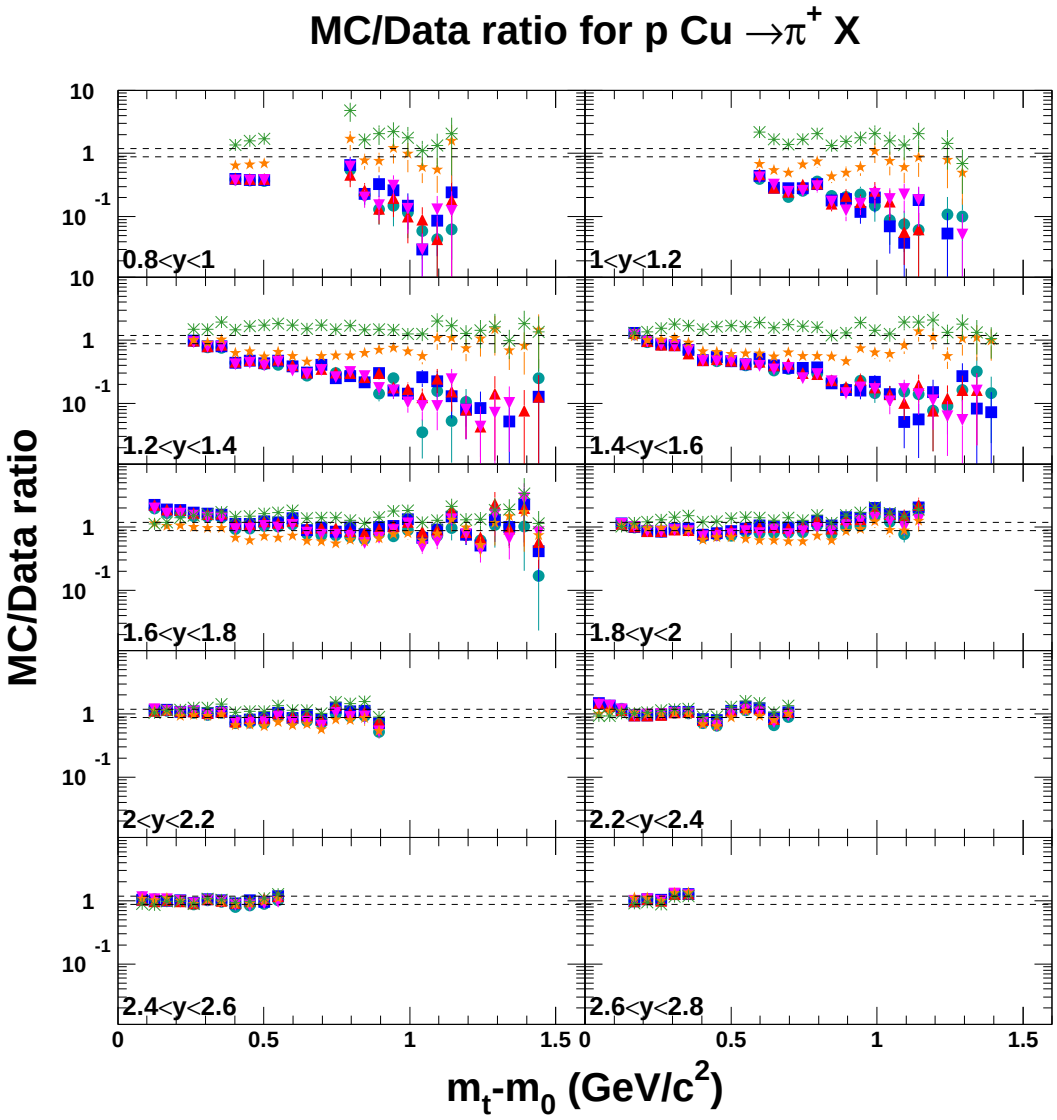


Fig. 9. The ratio of the simulated (MC) and data invariant cross sections as a function of transverse kinetic energy $m_t - m_0$ in 0.2 bins of rapidity for the $\pi^+$ data for $p$-Cu collisions. The horizontal dashed lines indicate the $\pm 15\%$ normalization uncertainty of the E802 data. The symbol definitions are the same as Figure 7.

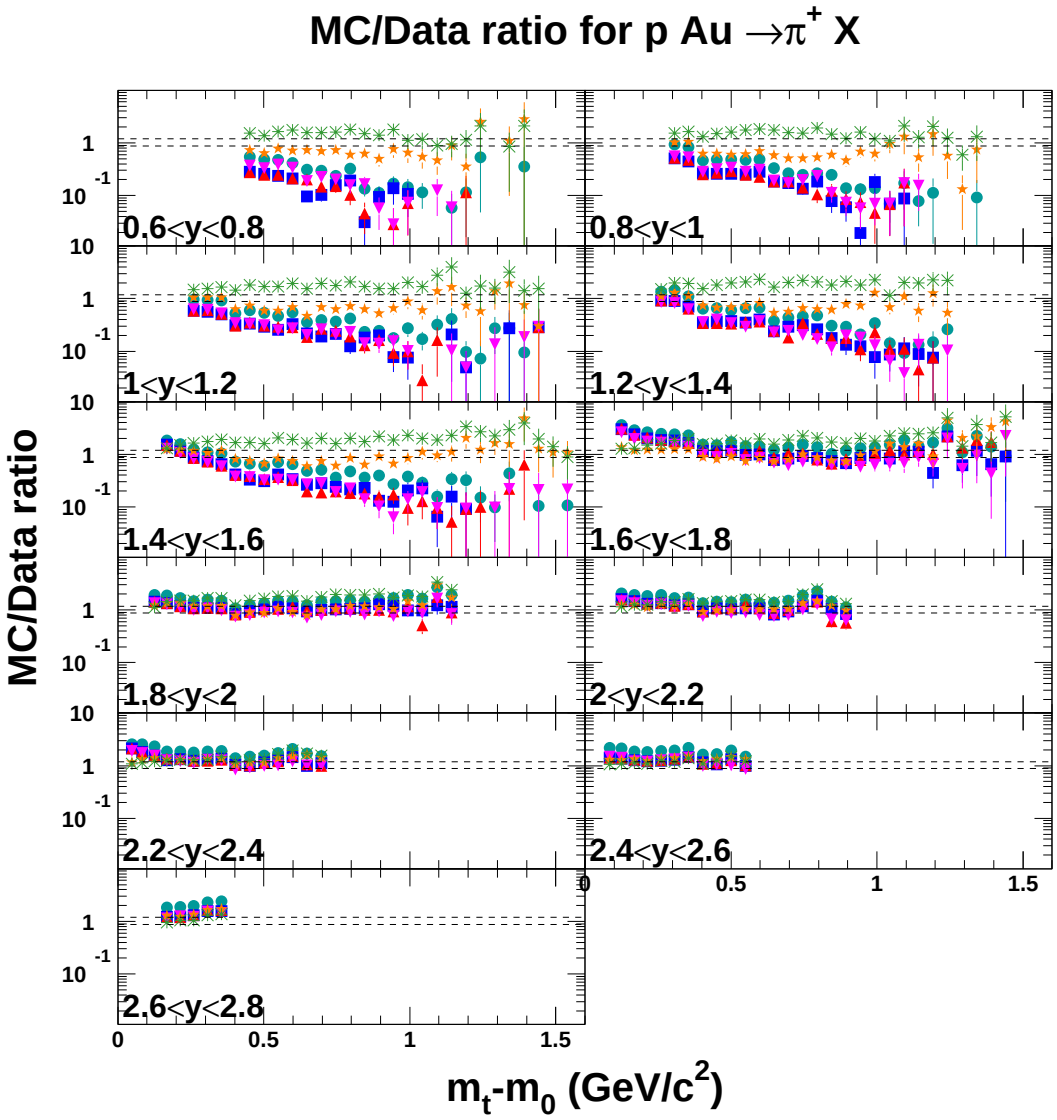


Fig. 10. The ratio of the simulated (MC) and data invariant cross sections as a function of transverse kinetic energy $m_t - m_0$ in 0.2 bins of rapidity for the $\pi^+$ data for $p$-Au collisions. The horizontal dashed lines indicate the $\pm 15\%$ normalization uncertainty of the E802 data. The symbol definitions are the same as Figure 7.

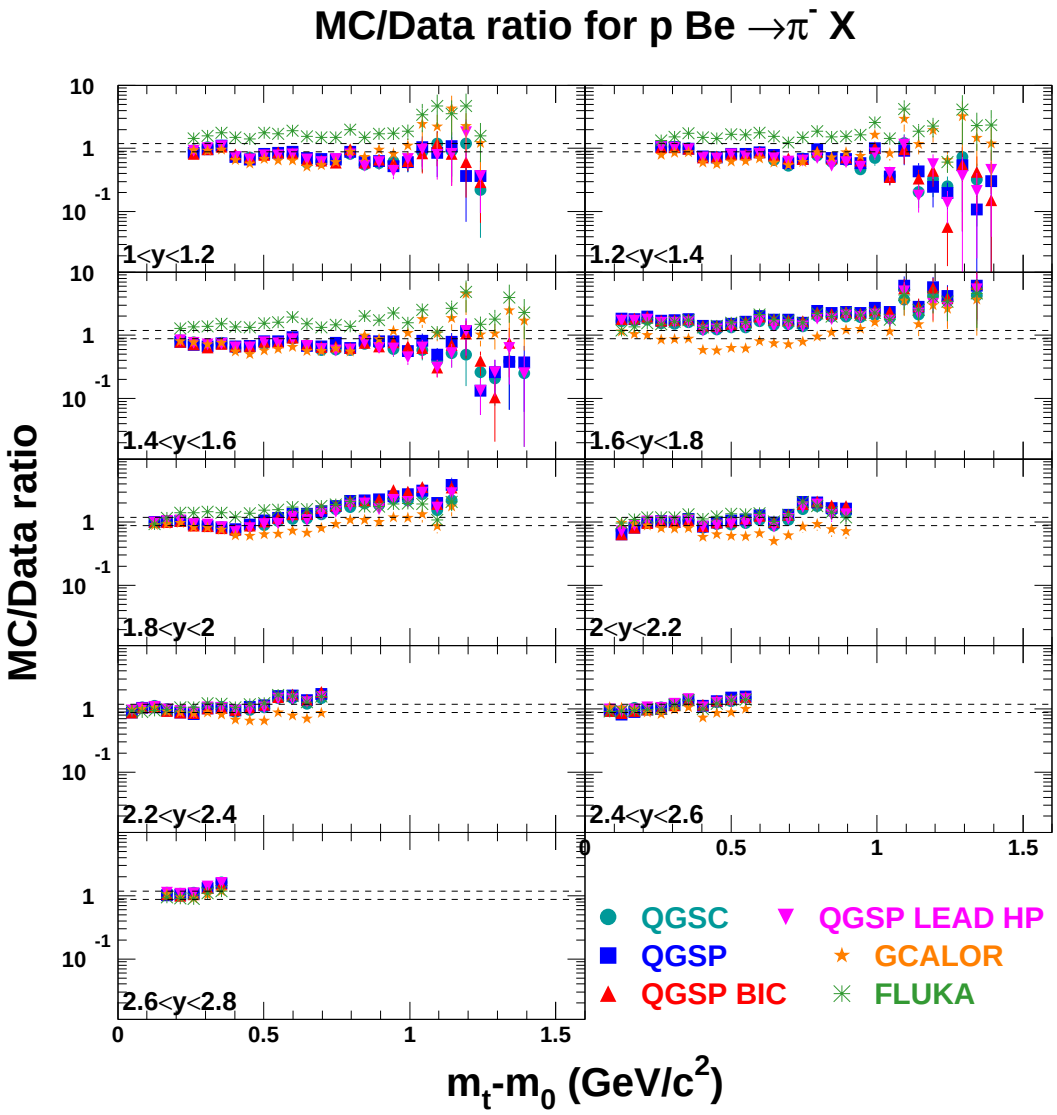


Fig. 11. The ratio of the simulated (MC) and data invariant cross sections as a function of transverse kinetic energy $m_t - m_0$ in 0.2 bins of rapidity for the $\pi^-$ data for $p$-Be collisions. The horizontal dashed lines indicate the $\pm 15\%$ normalization uncertainty of the E802 data.

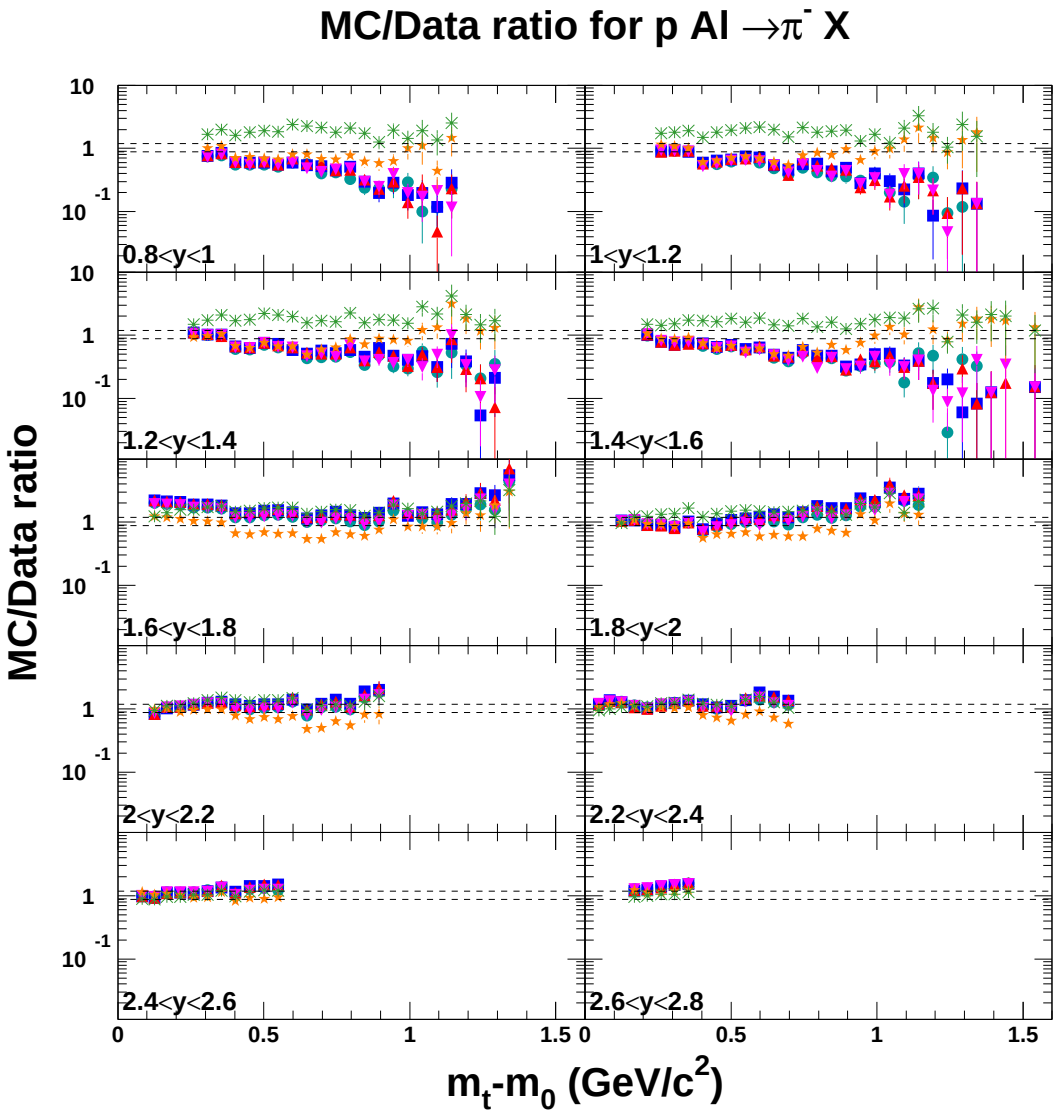


Fig. 12. The ratio of the simulated (MC) and data invariant cross sections as a function of transverse kinetic energy $m_t - m_0$ in 0.2 bins of rapidity for the $\pi^-$ data for $p$-Al collisions. The horizontal dashed lines indicate the $\pm 15\%$ normalization uncertainty of the E802 data. The symbol definitions are the same as Figure 11.

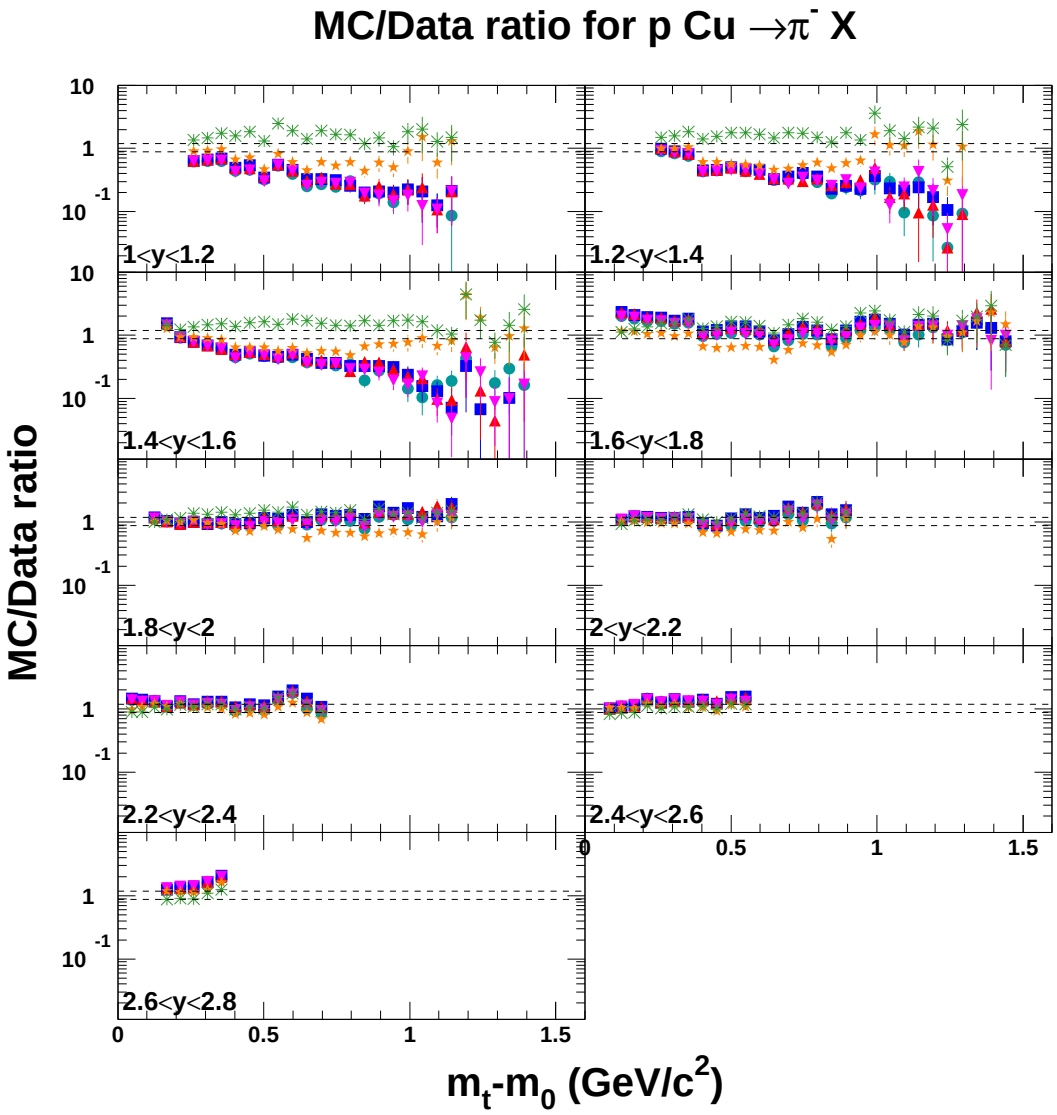


Fig. 13. The ratio of the simulated (MC) and data invariant cross sections as a function of transverse kinetic energy $m_t - m_0$ in 0.2 bins of rapidity for the $\pi^-$ data for $p$-Cu collisions. The horizontal dashed lines indicate the $\pm 15\%$ normalization uncertainty of the E802 data. The symbol definitions are the same as Figure 11.

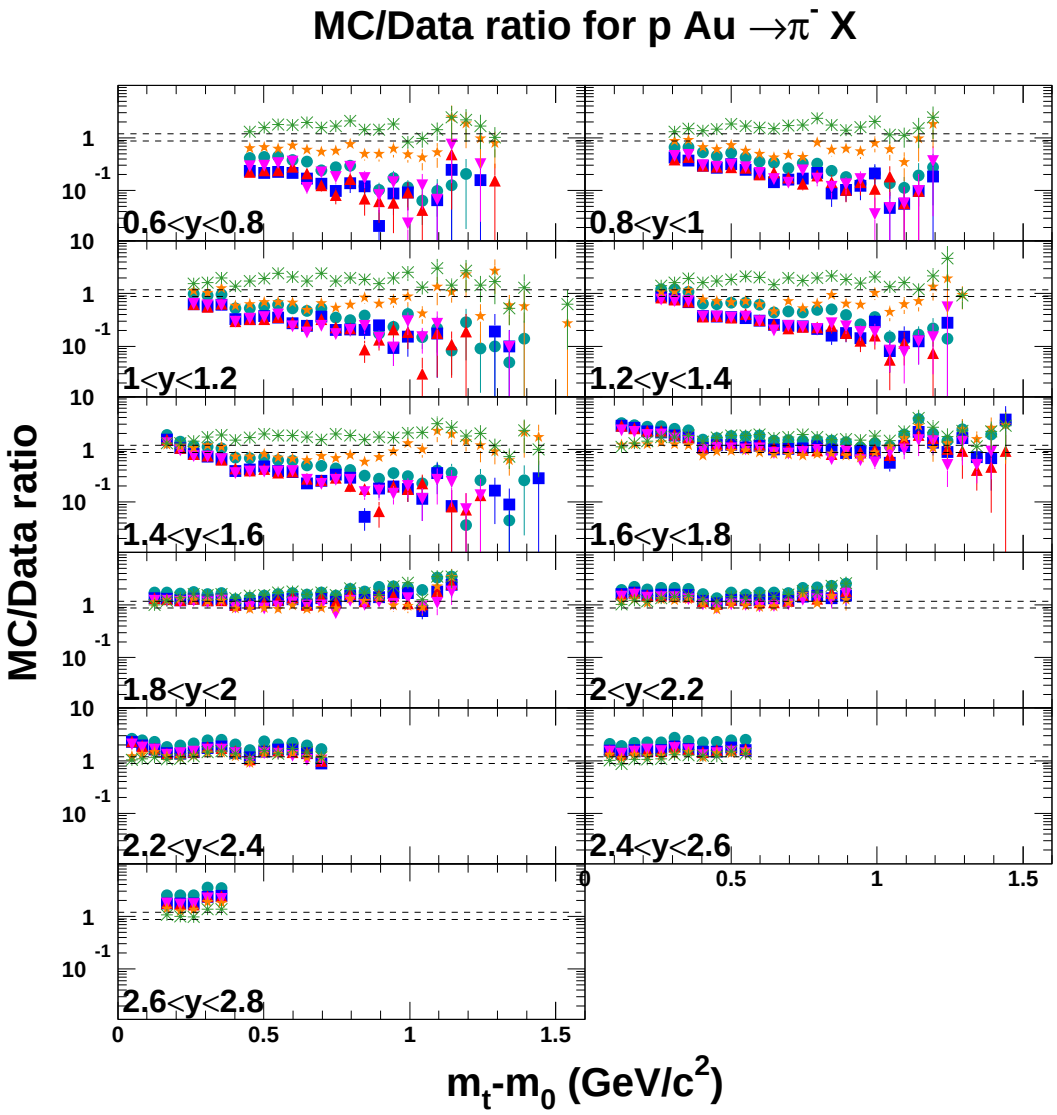


Fig. 14. The ratio of the simulated (MC) and data invariant cross sections as a function of transverse kinetic energy $m_t - m_0$ in 0.2 bins of rapidity for the $\pi^-$ data for $p$-Au collisions. The horizontal dashed lines indicate the $\pm 15\%$ normalization uncertainty of the E802 data. The symbol definitions are the same as Figure 11.

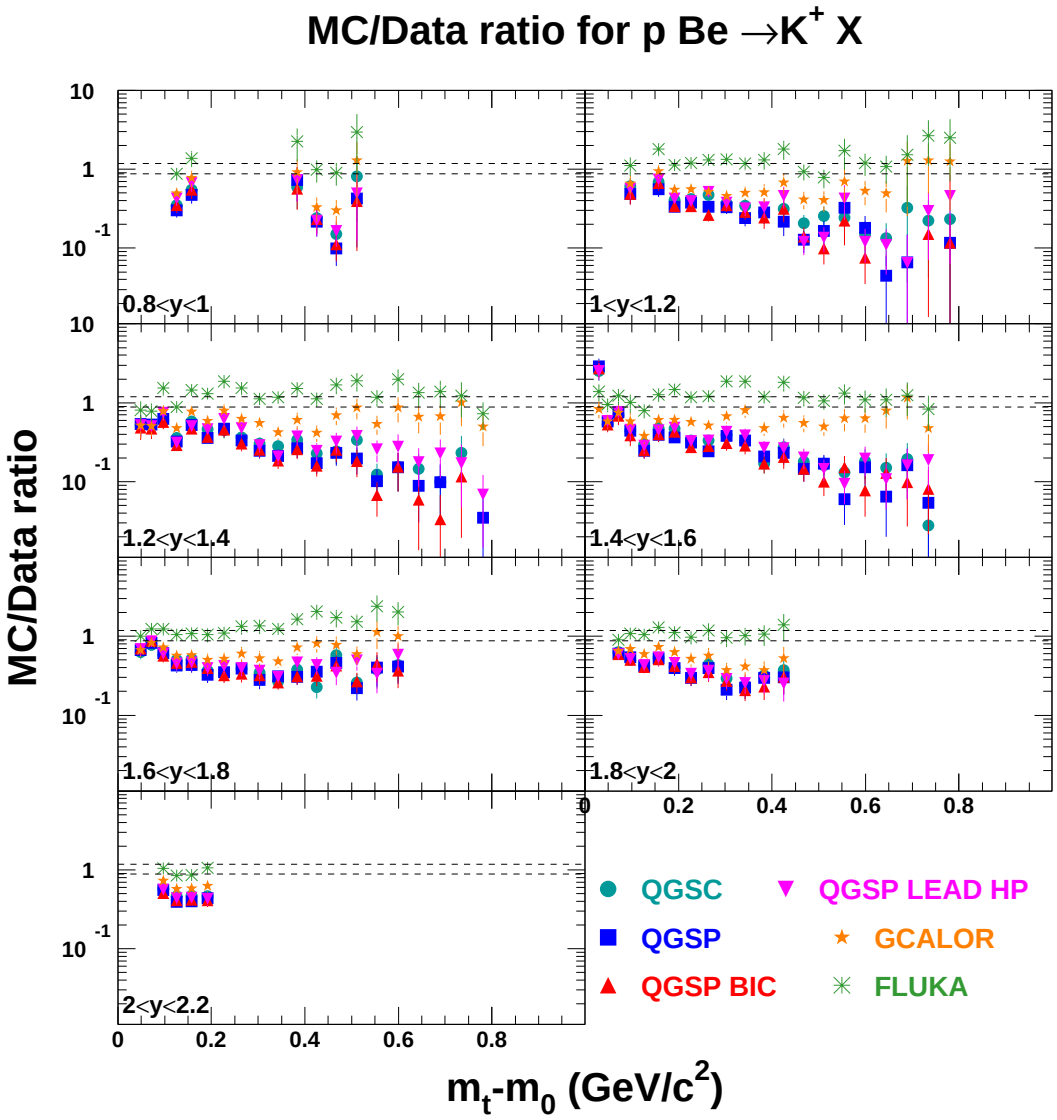


Fig. 15. The ratio of the simulated (MC) and data invariant cross sections as a function of transverse kinetic energy $m_t - m_0$ in 0.2 bins of rapidity for the $K^+$ data for $p$-Be collisions. The horizontal dashed lines indicate the $\pm 15\%$ normalization uncertainty of the E802 data.

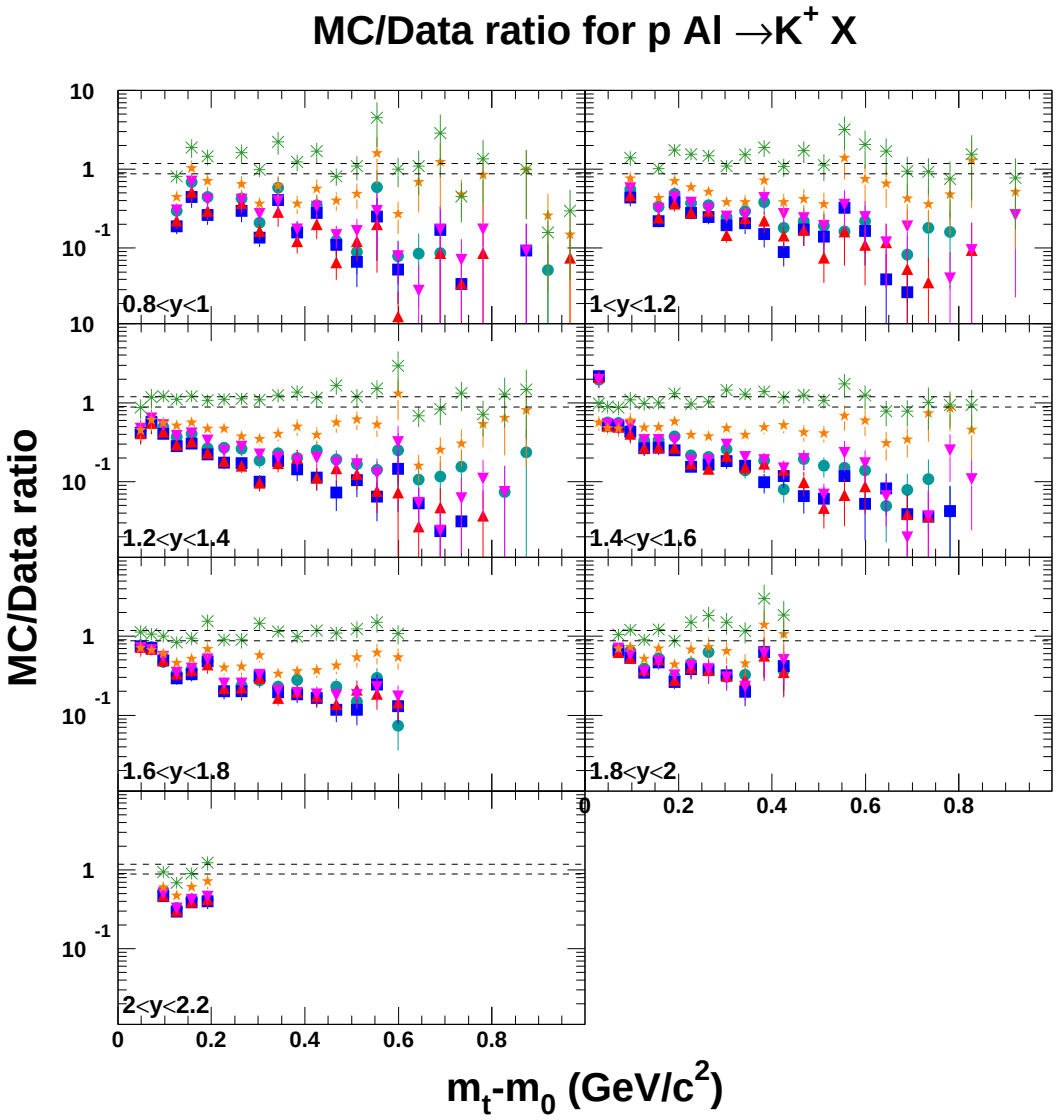


Fig. 16. The ratio of the simulated (MC) and data invariant cross sections as a function of transverse kinetic energy $m_t - m_0$ in 0.2 bins of rapidity for the $K^+$ data for $p$-Al collisions. The horizontal dashed lines indicate the $\pm 15\%$ normalization uncertainty of the E802 data. The symbol definitions are the same as Figure 15.

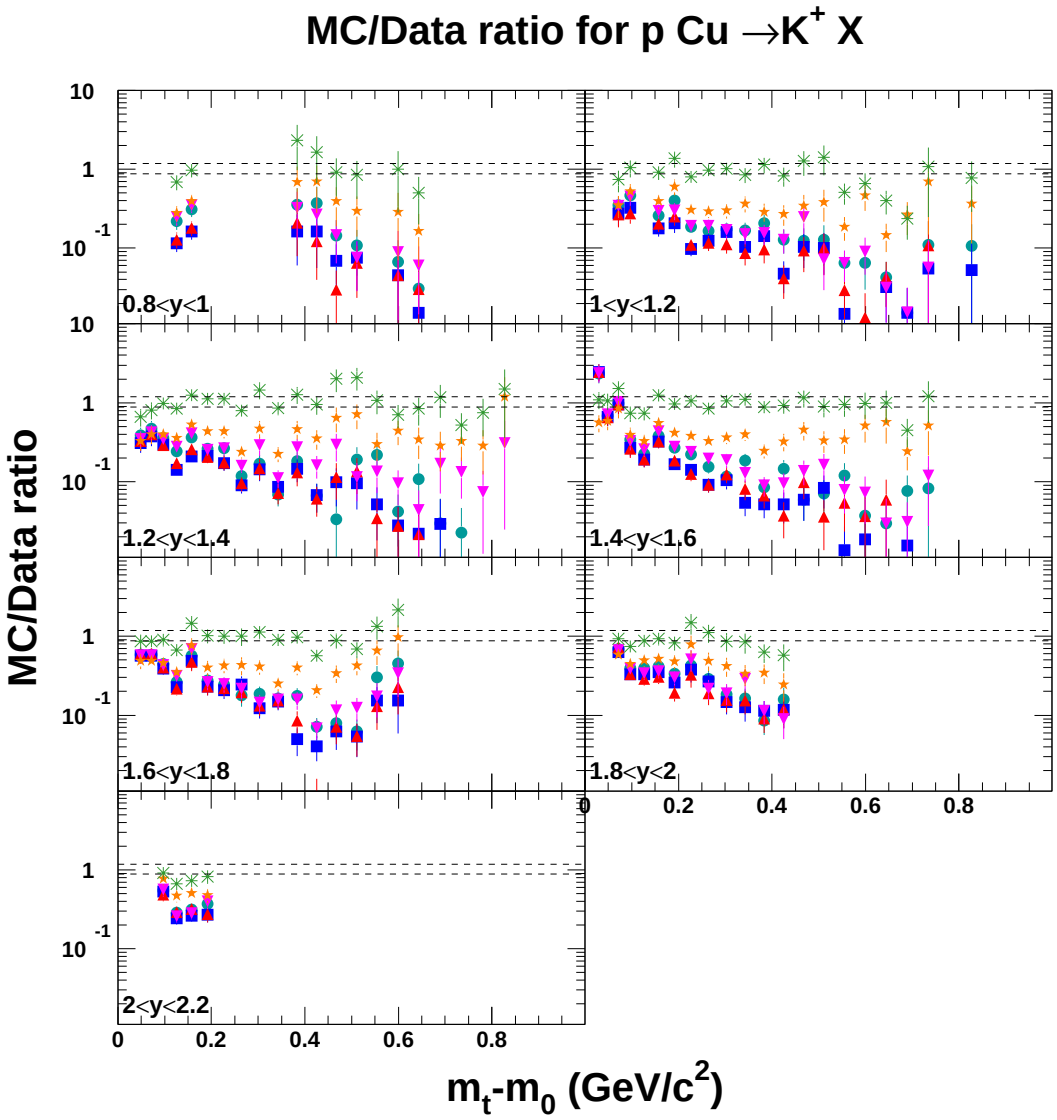


Fig. 17. The ratio of the simulated (MC) and data invariant cross sections as a function of transverse kinetic energy $m_t - m_0$ in 0.2 bins of rapidity for the $K^+$ data for $p$-Cu collisions. The horizontal dashed lines indicate the $\pm 15\%$ normalization uncertainty of the E802 data. The symbol definitions are the same as Figure 15.

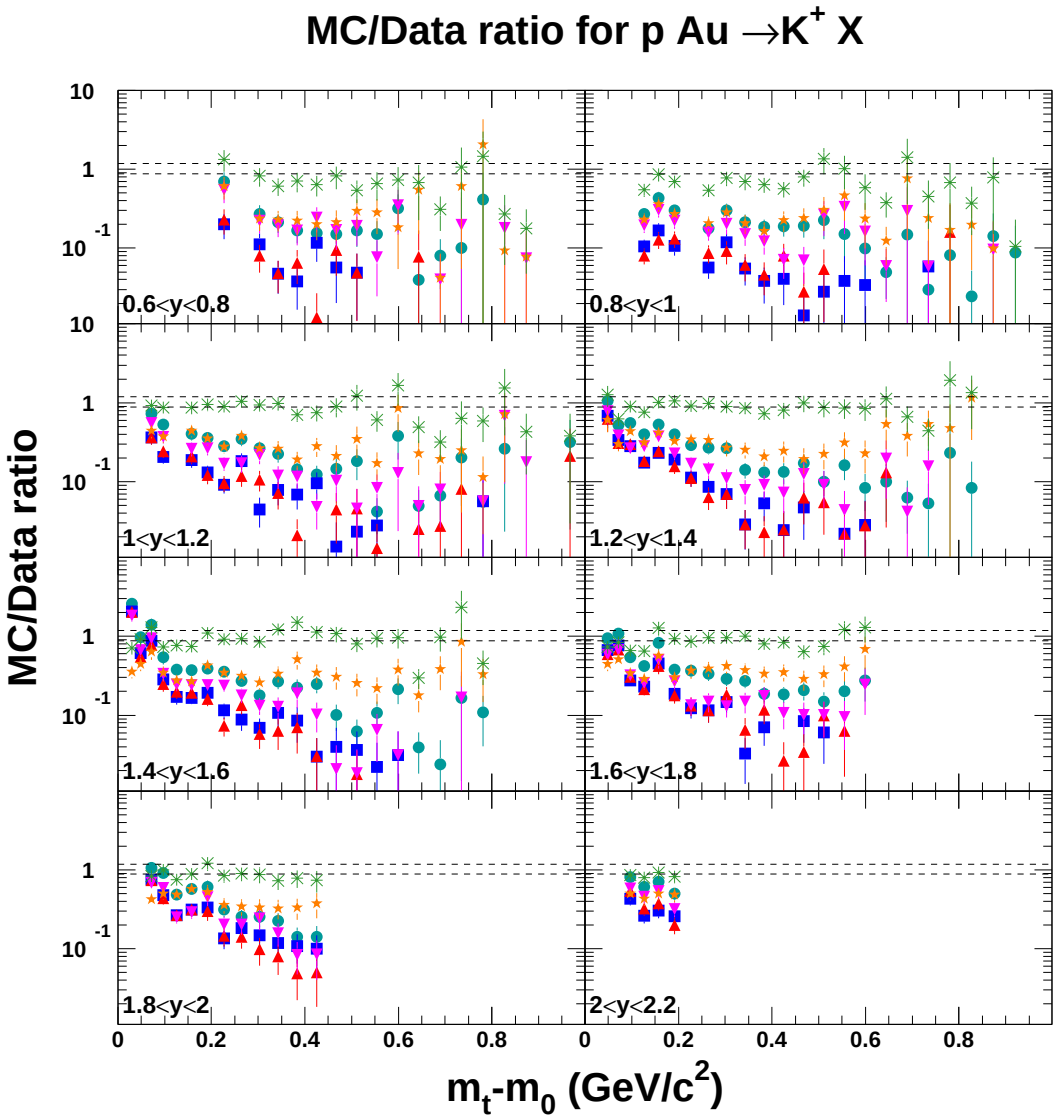


Fig. 18. The ratio of the simulated (MC) and data invariant cross sections as a function of transverse kinetic energy $m_t - m_0$ in 0.2 bins of rapidity for the $K^+$ data for $p$-Au collisions. The horizontal dashed lines indicate the $\pm 15\%$ normalization uncertainty of the E802 data. The symbol definitions are the same as Figure 15.

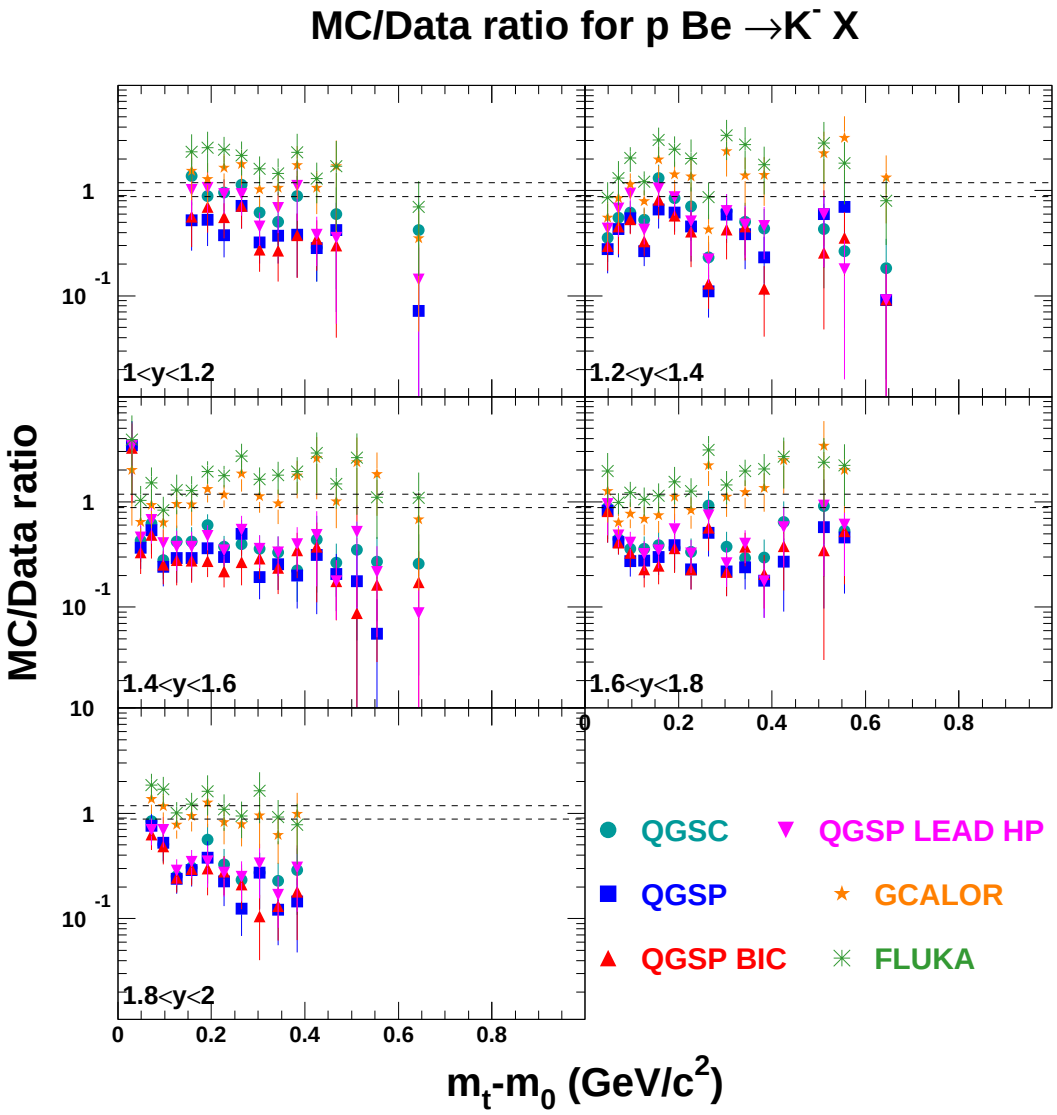


Fig. 19. The ratio of the simulated (MC) and data invariant cross sections as a function of transverse kinetic energy $m_t - m_0$ in 0.2 bins of rapidity for the $K^-$ data for $p$-Be collisions. The horizontal dashed lines indicate the $\pm 15\%$ normalization uncertainty of the E802 data.

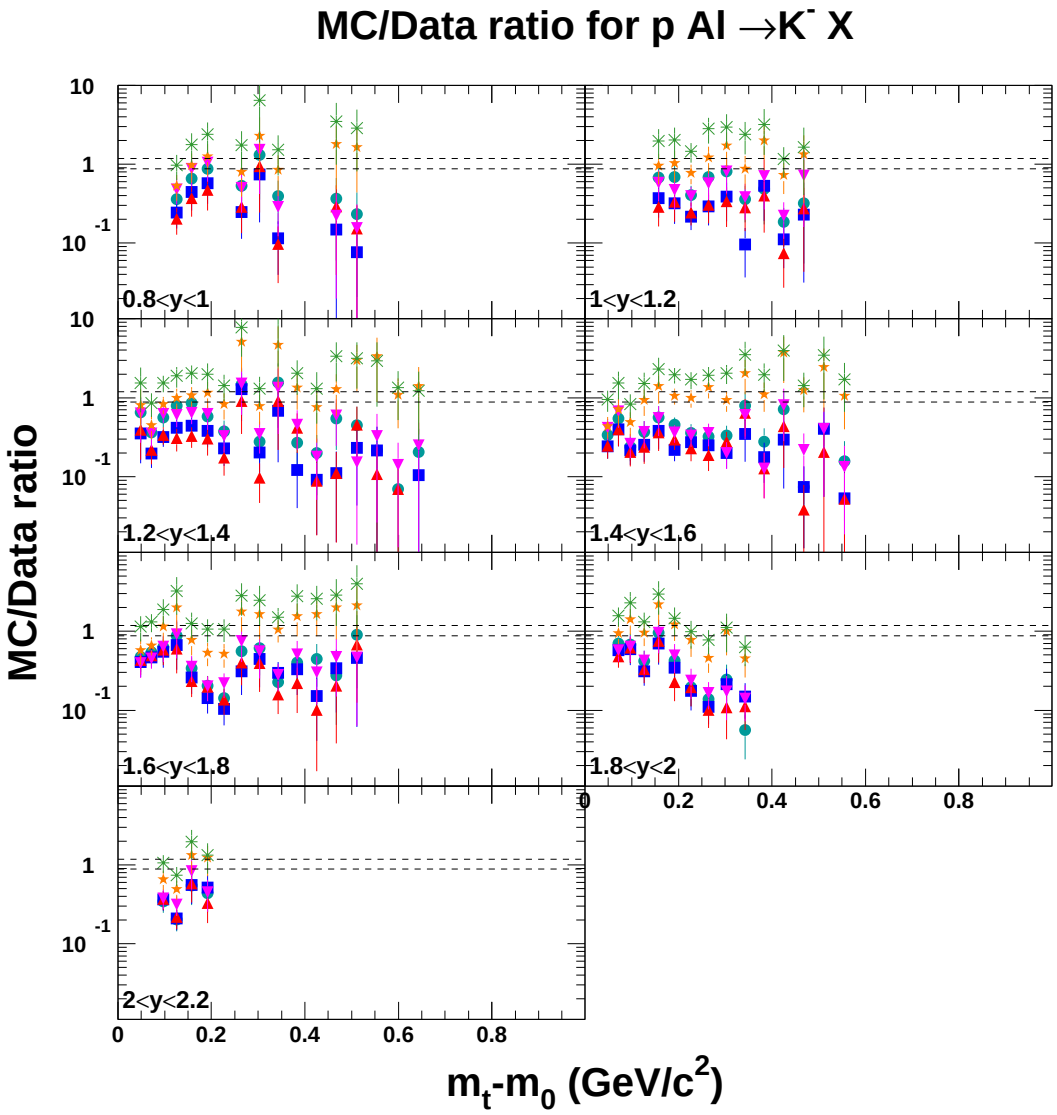


Fig. 20. The ratio of the simulated (MC) and data invariant cross sections as a function of transverse kinetic energy $m_t - m_0$ in 0.2 bins of rapidity for the $K^-$ data for $p$-Al collisions. The horizontal dashed lines indicate the $\pm 15\%$ normalization uncertainty of the E802 data. The symbol definitions are the same as Figure 19.

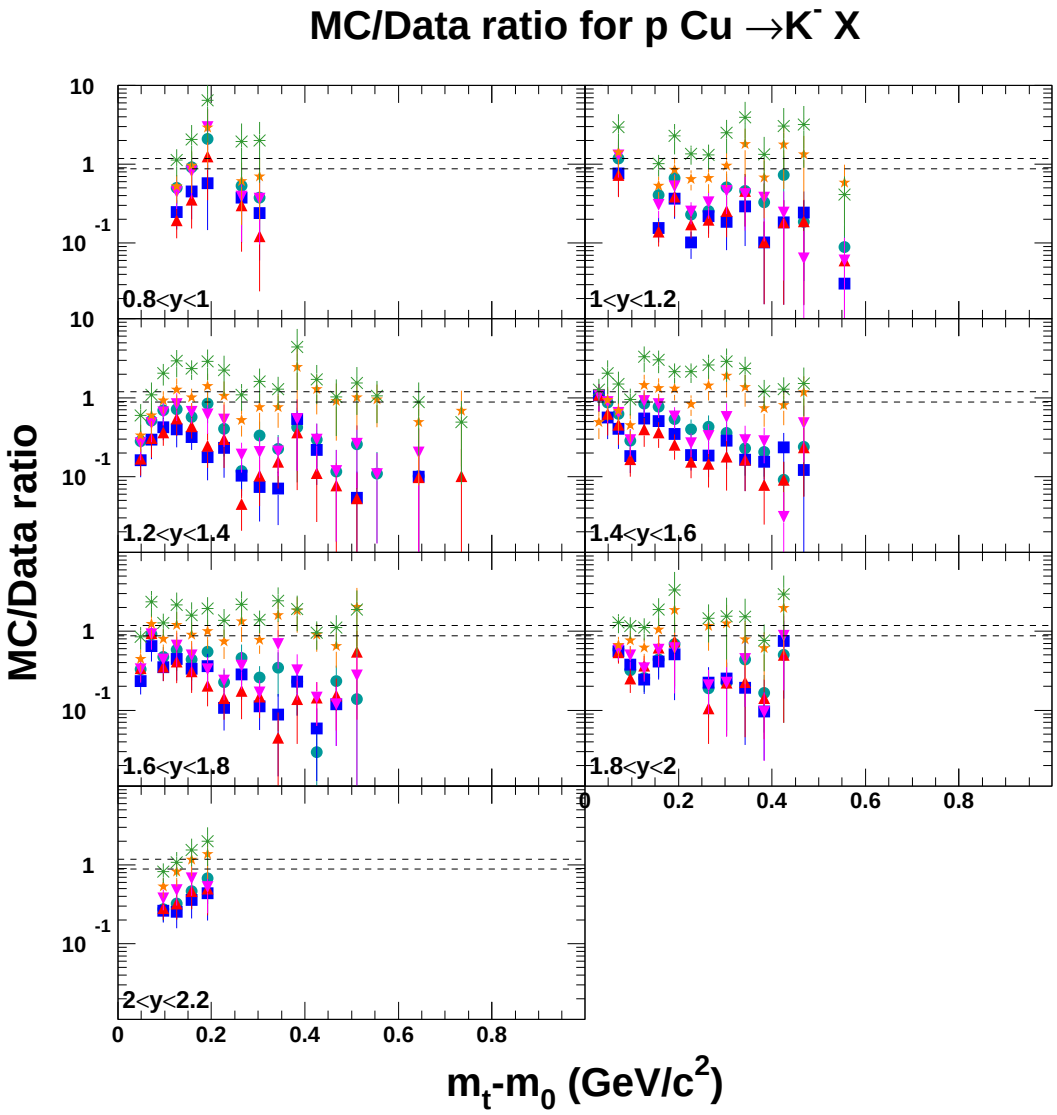


Fig. 21. The ratio of the simulated (MC) and data invariant cross sections as a function of transverse kinetic energy $m_t - m_0$ in 0.2 bins of rapidity for the $K^-$ data for $p$-Cu collisions. The horizontal dashed lines indicate the $\pm 15\%$ normalization uncertainty of the E802 data. The symbol definitions are the same as Figure 19.

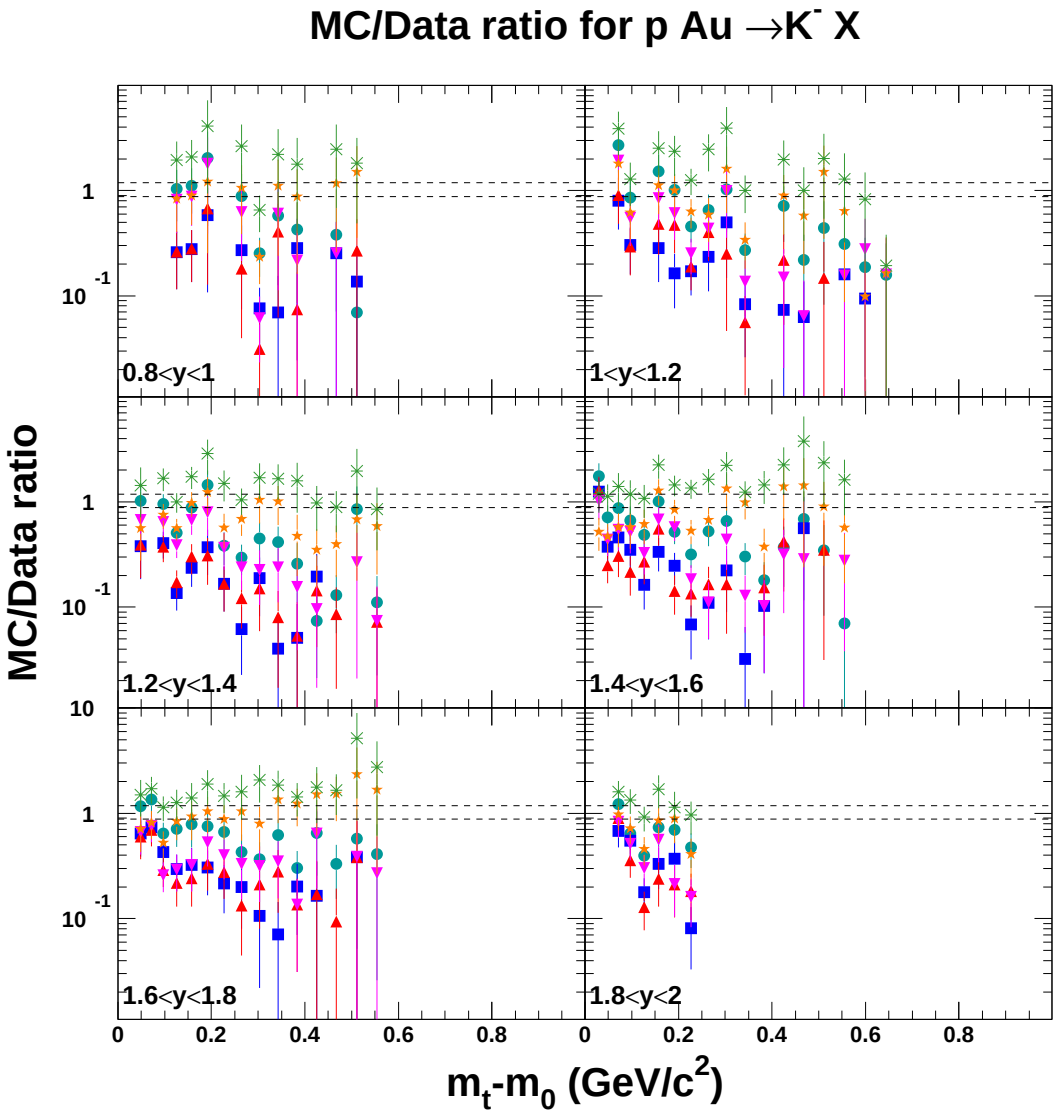


Fig. 22. The ratio of the simulated (MC) and data invariant cross sections as a function of transverse kinetic energy $m_t - m_0$ in 0.2 bins of rapidity for the $K^-$ data for $p$-Au collisions. The horizontal dashed lines indicate the $\pm 15\%$ normalization uncertainty of the E802 data. The symbol definitions are the same as Figure 19.

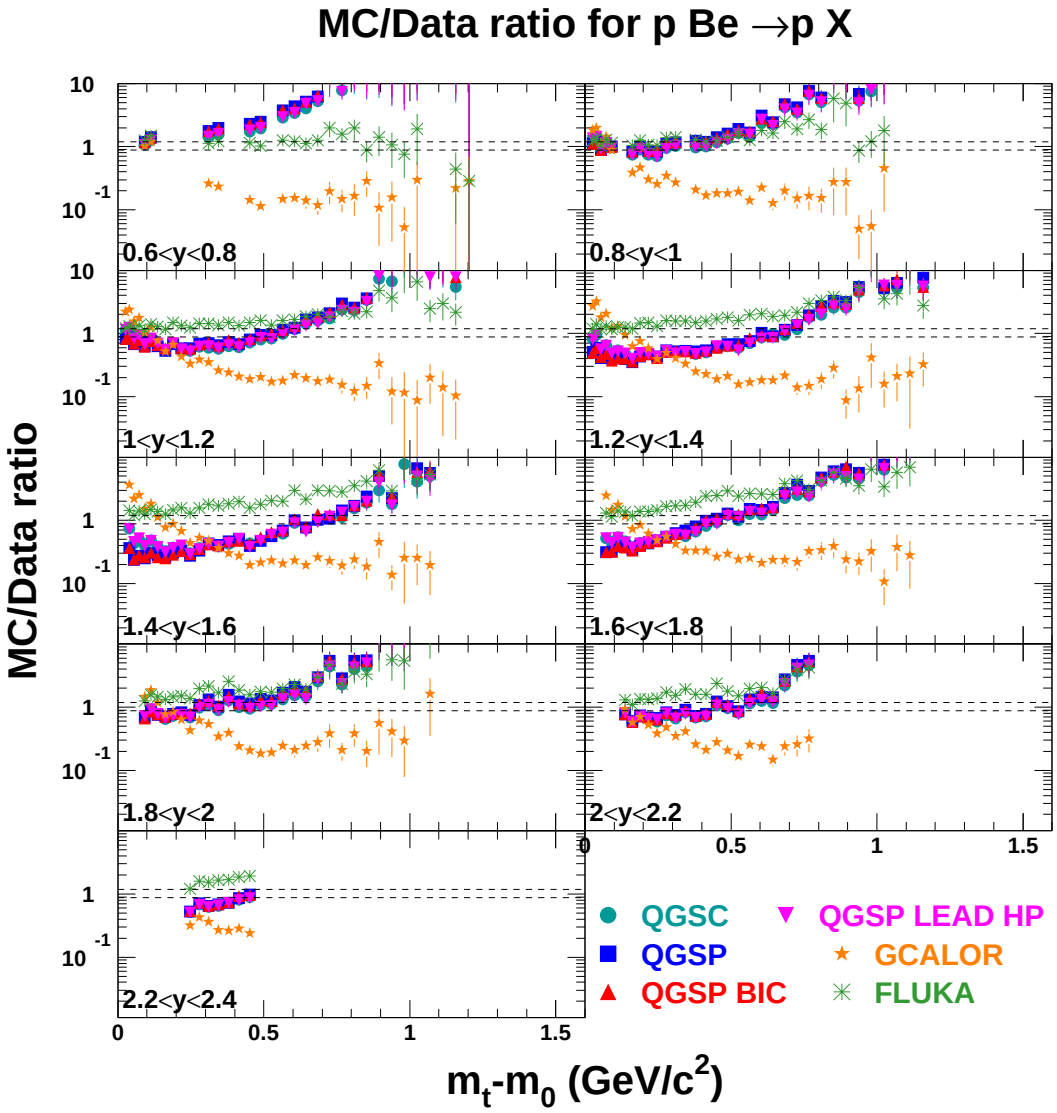


Fig. 23. The ratio of the simulated (MC) and data invariant cross sections as a function of transverse kinetic energy $m_t - m_0$ in 0.2 bins of rapidity for the proton data for $p$-Be collisions. The horizontal dashed lines indicate the $\pm 15\%$ normalization uncertainty of the E802 data.

## 4 Conclusions and discussion

The FLUKA simulation package gives the best overall agreement with the E802 meson data with the greatest deviation between the data and Monte Carlo of a factor of $\sim 2$ over the entire kinematic range of the data. The agreement of the GEANT3 and GEANT4 packages was worse in general. The agreement of all the simulation packages with the proton and deuteron production data was less satisfactory than that for the meson data.

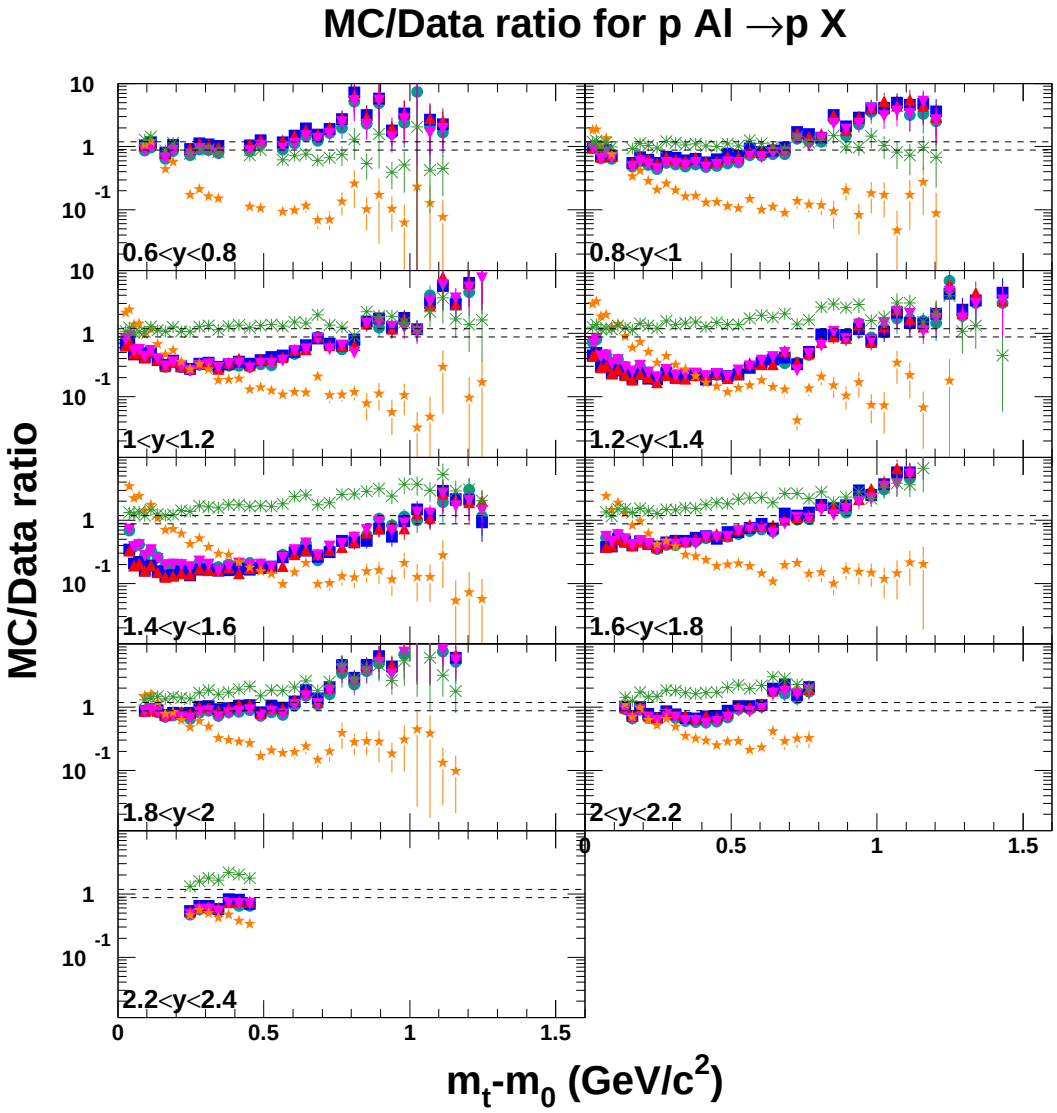


Fig. 24. The ratio of the simulated (MC) and data invariant cross sections as a function of transverse kinetic energy $m_t - m_0$ in 0.2 bins of rapidity for the proton data for $p$-Al collisions. The horizontal dashed lines indicate the $\pm 15\%$ normalization uncertainty of the E802 data. The symbol definitions are the same as Figure 23.

We note that a previous investigation with the JAM [9] simulation package gave good agreement and that JAM has been interfaced with GEANT4 [18] although there is no current plan to implement JAM as a hadronic physics list in GEANT4. In addition a great deal of data with similar targets and kinematics is currently being analyzed or accumulated [19] and should provide for validation and refinement of simulations.

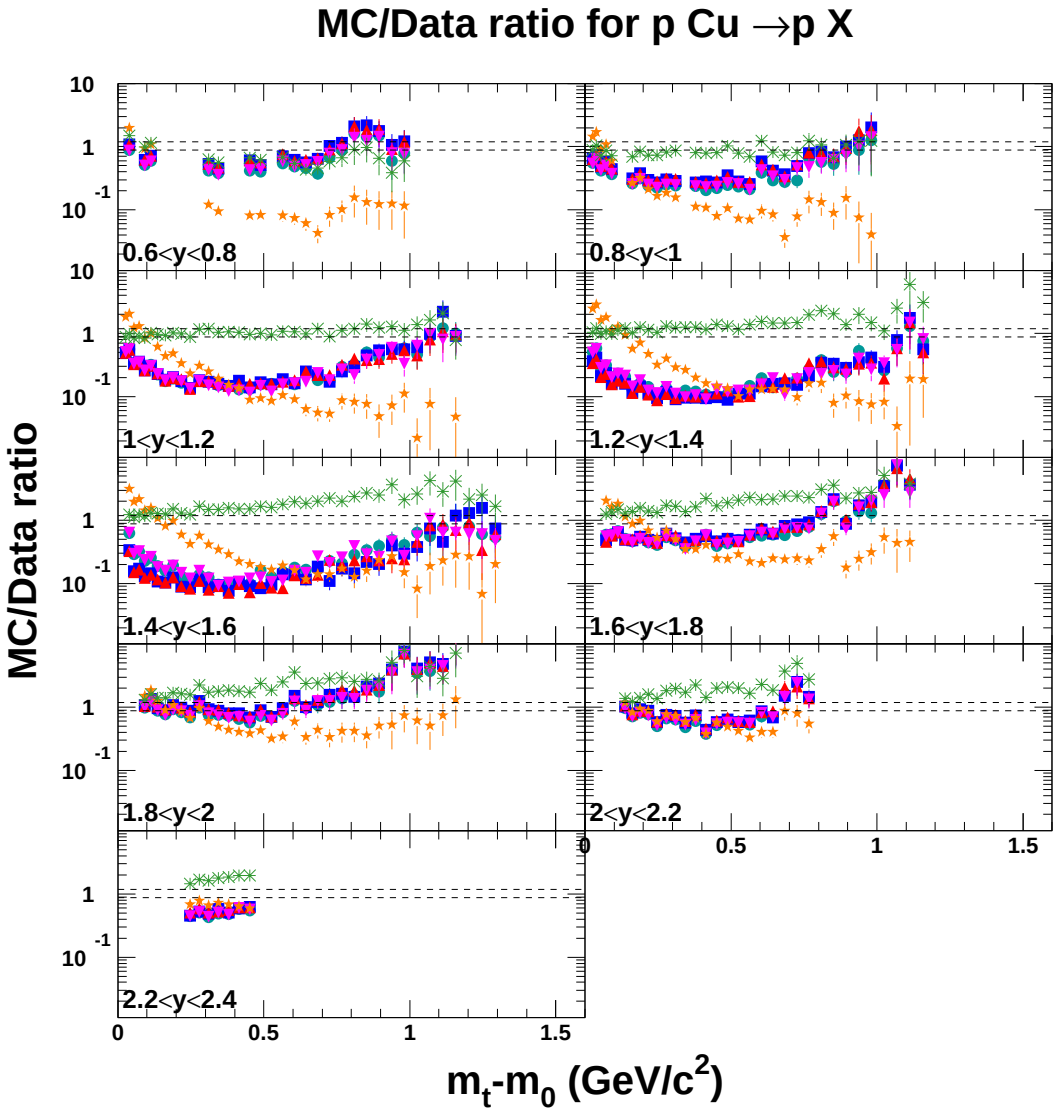


Fig. 25. The ratio of the simulated (MC) and data invariant cross sections as a function of transverse kinetic energy $m_t - m_0$ in 0.2 bins of rapidity for the proton data for $p$-Cu collisions. The horizontal dashed lines indicate the $\pm 15\%$ normalization uncertainty of the E802 data. The symbol definitions are the same as Figure 23.

## 5 Acknowledgements

We wish to thank Andrei Poblaguev for useful conversations and suggestions based on his earlier, unpublished comparisons of simulations with E802 data. We also thank Peter Gumplinger for assistance with the GEANT4 simulation. We acknowledge the assistance of E802 collaborators Dana Beavis, Chellis Chasman and Ramiro Debbe and Boris Pritychenko of the National Nuclear Data Center in locating the tables of the E802 results.

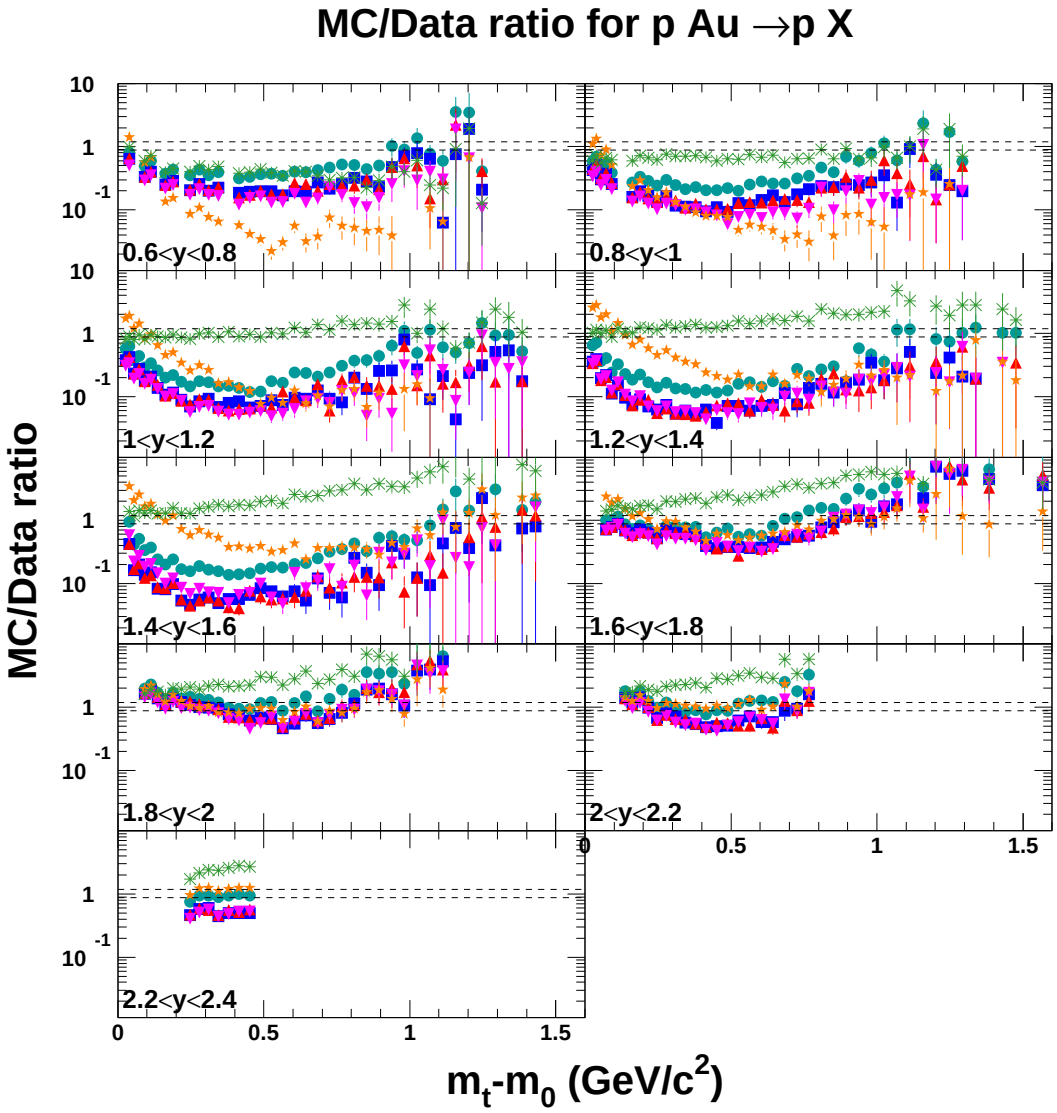


Fig. 26. The ratio of the simulated (MC) and data invariant cross sections as a function of transverse kinetic energy $m_t - m_0$ in 0.2 bins of rapidity for the proton data for $p$-Au collisions. The horizontal dashed lines indicate the $\pm 15\%$ normalization uncertainty of the E802 data. The symbol definitions are the same as Figure 23.

This manuscript was authored by Brookhaven Science Associates, LLC under Contract No. DE-AC02-98CH1-886 with the U.S. Department of Energy. The United States Government retains, and the publisher, by accepting the article for publication, acknowledges, a world-wide license to publish or reproduce the published form of this manuscript, or allow others to do so, for the United States Government purposes.

This work was partially funded by National Science Foundation Grant #0428662 to NYU for RSVP Advanced Planning.

## References


[1] Todor Stanev, Nucl.Phys.Proc.Suppl. **145**, 69 (2005).

[2] A. Guglielmi, Phys. Atom. Nucl. **65**, 2202 (2002) [Yad. Fiz. **65**, 2265 (2002)].

[3] D. A. Bryman and L. Littenberg, Nucl. Phys. Proc. Suppl. **99B**, 61 (2001).

[4] A.De Roeck, F.Gianotti, A. Morsch and W.Pokorski, CERN-LCGAPP-2004-02.

[5] T. Abbott *et al.*, Phys.Rev. **D45**, 3906 (1992).

[6] GEANT, CERN Program Library Long Writeup W5013, Copyright CERN, Geneva 1993; `http://wwwasdoc.web.cern.ch/wwwasdoc/geant_html3/geantall.html`.

[7] S. Agostinelli *et al.* [GEANT4 Collaboration], Nucl. Instrum. Meth. A **506**, 250 (2003); `http://wwwasd.web.cern.ch/wwwasd/geant4/`.

[8] A. Fassó, A. Ferrari, P. R. Sala and J. Ranft, SLAC-REPRINT-2000-117 *Prepared for International Conference on Advanced Monte Carlo for Radiation Physics, Particle Transport Simulation and Applications (MC 2000), Lisbon, Portugal, 23-26 Oct 2000*; A. Fassó, A. Ferrari and P. Sala, SLAC-REPRINT-2000-116 *Prepared for International Conference on Advanced Monte Carlo for Radiation Physics, Particle Transport Simulation and Applications (MC 2000), Lisbon, Portugal, 23-26 Oct 2000*; `http://pcfluka.mi.infn.it/`.

[9] Y. Nara, N. Otuka, A. Ohnishi, K. Niita and S. Chiba, Phys. Rev. C **61**, 024901 (2000) [arXiv:nucl-th/9904059].

[10] G. Battistoni, A. Ferrari, T. Montaruli and P. R. Sala, Astropart. Phys. **19**, 269 (2003) [Erratum-ibid. **19**, 291 (2003)] [arXiv:hep-ph/0207035].

[11] D. Heck, arXiv:astro-ph/0410735.

[12] S. A. Bass *et al.*, Prog. Part. Nucl. Phys. **41**, 225 (1998) [arXiv:nucl-th/9803035].

[13] H. J. Drescher, M. Hladik, S. Ostapchenko, T. Pierog and K. Werner, Phys. Rept. **350**, 93 (2001) [arXiv:hep-ph/0007198].

[14] H. Fesefeldt, PITHA-85-02

[15] N. N. Kalmykov, S. S. Ostapchenko and A. I. Pavlov, Nucl. Phys. Proc. Suppl. **52B**, 17 (1997).

[16] C. Zeitnitz and T. A. Gabriel, Nucl. Instrum. Meth. A **349**, 106 (1994); `http://www.staff.uni-mainz.de/zeitnitz/Gcalor/gcalor.html`.

[17] `http://wwwasd.web.cern.ch/wwwasd/geant4/physics_lists/`

[18] T. Koi, M. Asai, D. H. Wright, K. Niita, Y. Nara, K. Amako and T. Sasaki, eConf **C0303241**, THMT005 (2003) [arXiv:physics/0306115].

[19] G. Barr and R. Engel, arXiv:astro-ph/0504356.